From DEPARTMENT OF NEUROSCIENCE
Karolinska Institutet, Stockholm, Sweden

GENERATION AND INVESTIGATION OF NEURAL MICROENVIRONMENT IN HEALTH AND DISEASE

Jakub Lewicki

Karolinska Institutet

Stockholm 2019

Published by Karolinska Institutet.
Printed by Eprint AB 2019

ISBN 978-91-7831-566-6

Generation and investigation of neural microenvironment in health and disease

THESIS FOR DOCTORAL DEGREE (Ph.D.)

ACADEMIC DISSERTATION
For the degree of PhD at Karolinska Institutet

This thesis will be defended in public at the Inghesalen Lecture Hall, Tomtebodavägen 18, Karolinska Institutet, Stockholm, Sweden

Friday the 1st of November, 2019, 9:30

By

Jakub Lewicki

Principal Supervisor:
Dr. Ola Hermanson
Karolinska Institutet
Department of Neuroscience

Co-supervisor(s):
Professor Bertrand Joseph
Karolinska Institutet
Institute of Environmental Medicine

Opponent:
Dr. Yu Shrike Zhang
Harvard Medical School
Department of Medicine

Examination Board:
Dr. Jan-Bernd Stukenborg
Karolinska Institutet
Department of Women's and Children's Health

Dr. Roman Chrast
Karolinska Institutet
Department of Neuroscience

Dr. Gemma Mestres Beà
Uppsala University
Department of Engineering Sciences

“The only difference between screwing around and science is writing it down”

Adam Savage

ABSTRACT

Cells in our body are under the constant influence of intrinsic and extrinsic factors that modulate their behavior. Early on, starting during the development of the organism, growth factors, nutrients, oxygen, the extracellular matrix and contact with other cells affect essential processes such as proliferation, migration, differentiation and apoptosis. Later on, the same types of stimuli regulate tissue homeostasis and play important roles in disease onset. Although our understanding of the cellular microenvironment and its impact on the cells is deeper than ever before, we still do not fully understand the whole complexity behind it, making the need to not only study the microenvironment but also replicate it *in vitro* more pressing. Areas such as tissue engineering, disease modeling, drug testing and *in vitro* microphysiological systems are just some examples where new knowledge and tools in this field are necessary for progress.

This thesis reflects the path I took to first study and then to recreate some of the aspects of the neural microenvironment. Paper I is a study of the redox sensing co-repressor CtBP2. This protein is well known to integrate oxygen levels and regulate gene expression during development and disease. When knocked down in the mouse embryonic brain, normal cortex formation was disrupted, revealing an important role of CtBP2 in neural stem cell maintenance, differentiation, and migration. In Paper II, we focused on CtBP2 at the molecular level, studying it *in vitro* in rat neural stem cells (NSCs). By applying different metabolic conditions *in vitro*, we showed that hypoxia and 2-Deoxy-D-glucose increased acetylation of CtBP2 in proliferating NSCs. Additionally, 1% oxygen treatment resulted in altered homodimerization of CtBP2 showing that some aspects of the NSC environment are conveyed to post-translational modifications of CtBP2, an important step in its functional regulation.

Paper III explores the use of 3D bioprinting technology and a special material deposition technique – freeform reversible embedding of suspended hydrogels (FRESH) – to generate a relevant microenvironment for human neuroblastoma 3D cell culture. Using a Parameter Optimization Index (POI), we optimized sodium alginate (SA) printing parameters including extrusion pressure and speed. With this approach, we successfully printed human neuroblastoma cells in 3D encapsulated in SA, maintaining good cell viability and high print quality.

Lastly, to find a more robust biomaterial for the *in vitro* microenvironment engineering for human neuroepithelial-like stem cells (NESCs), in Paper IV we investigated the cytocompatibility of these cells with vitronectin-modified recombinant spider silk (VN-NT2RepCT). Our study showed the necessity of spider silk functionalization with vitronectin to provide attachment for NESCs. This material successfully supported neural stem cell growth and proliferation, and further analysis of the morphology of focal adhesions revealed differences in cell attachment compared to control substrates. Our results suggest potential applications for the VN-NT2RepCT in tissue engineering, possibly including 3D bioprinting.

LIST OF SCIENTIFIC PAPERS

I. Karaca E, Li X, **Lewicki J**, Neofytou C, Guérout N, Barnabé-Heider F, Hermanson O, The corepressor CtBP2 is essential for proper development of the mouse cortex. *Manuscript*

II. Karaca E, **Lewicki J**, Hermanson O (2014) Oxygen-dependent acetylation and dimerization of the corepressor CtBP2 in neural stem cells. *Exp Cell Research* 332, 128–135

III. **Lewicki J**, Bergman J, Kerins C, Hermanson O (2019) Optimization of 3D bioprinting of human neuroblastoma cells using sodium alginate hydrogel. *Bioprinting* 16

IV. **Lewicki J**, Bakker R, Johansson J, Nordling K, Rising A, Hermanson O, Cytocompatibility study of vitronectin-modified recombinant spider silk for human neuroepithelial stem cells culture. *Manuscript*

CONTENTS

LIST OF ABBREVIATIONS

2D	two-dimensional
2DG	2-Deoxy-D-glucose
3D	three-dimensional
bHLH	basic helix-loop-helix
CP	cortical plate
CR	Cajal-Retzius
CtBP	C-terminal-binding protein
DL	deep layer
E	embryonic day
ECM	extracellular matrix
FA	focal adhesion
FGF	fibroblast growth factor
FRESH	freeform reversible embedding of suspended hydrogels
GABA	gamma-aminobutyric acid
HDAC	histone deacetylase
HIF	hypoxia-inducible factor
IZ	intermediate zone
MSC	mesenchymal stem cell

NAD	nicotinamide adenine dinucleotide
NB	neuroblastoma
NEC	neuroepithelial cell
NESC	neuroepithelial-like stem cell
NSC	neural stem cell
PLA	proximity ligation assay
POI	parameter optimization index
RGC	radial glial cells
SA	sodium alginate
SVZ	subventricular zone
UL	upper layer
VZ	ventricular zone

1 INTRODUCTION

1.1 CORTICAL DEVELOPMENT

The cerebral cortex is composed of two main types of neurons: excitatory glutamatergic pyramidal neurons and inhibitory GABAergic interneurons releasing the neurotransmitter gamma-aminobutyric acid (GABA). Pyramidal cells constitute approximately 80% of all cortical neurons and establish local connections between cortical areas as well as project to other subcortical regions [1]. They originate in the proliferative ventricular zone of the dorsal telencephalon and migrate radially to the cortical plate forming different cortical layers [2]. GABAergic neurons, on the other hand, are a group of cells that originate in ganglionic eminence and migrate tangentially to occupy specific layers and establish local circuits in the cortex [3,4].

The development of the cerebral cortex is initiated with the closure of the neural tube at embryonic day (E) 10 in mouse and E26-28 in human when dividing neuroepithelial cells (NECs) form the ventricular zone (VZ) (see Figure 1 for the visualization of cortex development from this point). Initially a series of symmetrical divisions of NECs increases the thickness of the VZ expanding stem cell pool. Neurogenesis starts when NECs begin asymmetric divisions giving rise to one progenitor and one post-mitotic cell that eventually differentiates into either neuronal or glial cell [5,6]. The progenitor cells generated by NECs called radial glial cells (RGC) have the characteristic morphology of apical and basal processes that extend between the ventricular and pial surface and commonly display Nestin, PAX6, and RC2 among other marker proteins [7]. Initially RGCs undergo asymmetric divisions generating a projection neuron and another RGC in a process termed direct neurogenesis.

Over time, RGCs give rise to intermediate progenitors (IPs) that start to accumulate above the VZ creating a subventricular zone (SVZ) [8,9]. These progenitor cells express among others TBR2, CUX1, and CUX2 [10,11]. Most IPs will follow symmetrical division giving rise to two neurons [12]. The first generated neurons start forming the preplate. Later, more neurons start migrating forming cortical layers in an inside-out fashion, from deep layers (DL, V-VI) occupied by earliest-born neurons to upper layers (UL, II-IV) constituted of late-born neurons. Neurons from layers V-VI express transcription factors such as CTIP2 (BLC11B) and TBR1 [13–15] whereas neurons from layers II-III typically express CUX1/2, BRN1/2 and SATB2 [11,16,17]. Cortical neurogenesis finishes during prenatal development (E18.5 in mouse, embryonic week 27 in human) with subsequent gliogenesis taking place shortly after birth [18].

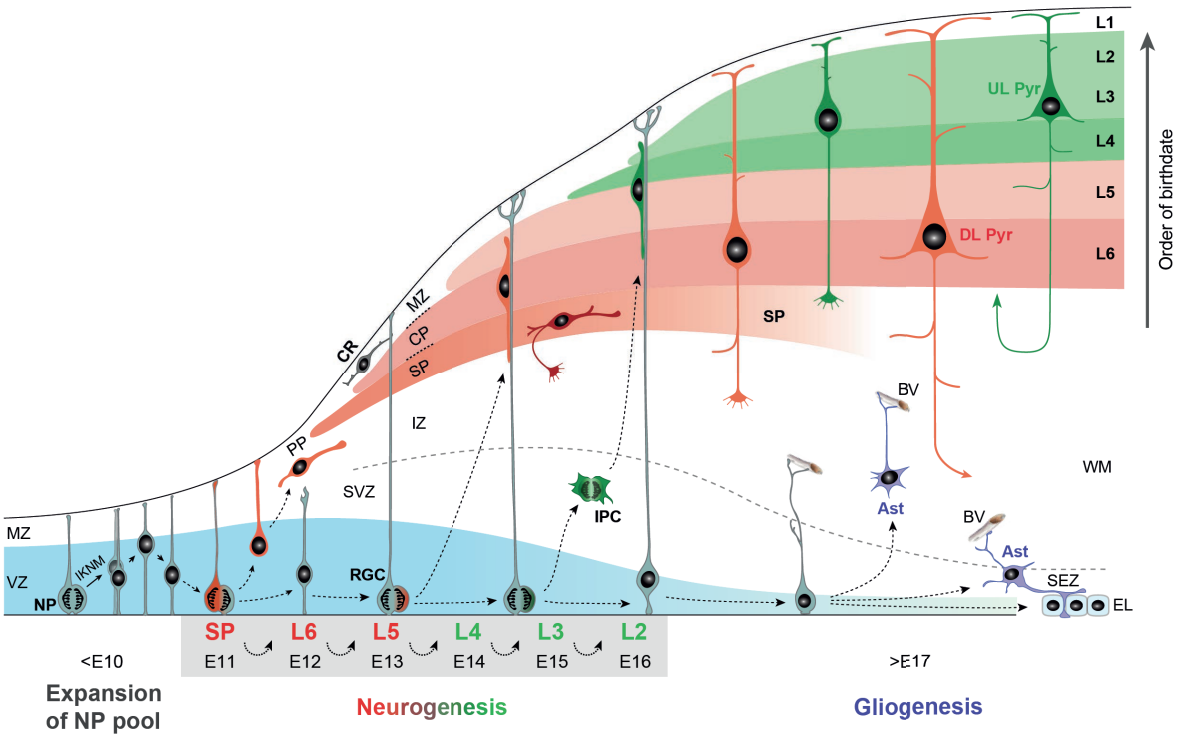

Figure 1. **Schematic representation of mouse neocortical development**. Reproduced from Kwan et al. (2012) with permission from the Company of Biologists. Early during neural development, the progenitor pool is expanded by neural progenitors (NPs) by symmetric divisions in the ventricular zone (VZ). In their cell cycle, NPs undergo interkinetic nuclear migration (IKNM) when the nucleus moves between the apical and basal surface. At E11.5, NPs start dividing asymmetrically, generating neurons which start to migrate upwards guided by radial glia cells (RGC). The preplate (PP) is formed by the arrival of the first projection neurons, the first step in the development of the cortical plate (CP). The PP is later divided into the marginal zone (MZ) and the subplate (SP) by more neurons migrating to the area. NPs continue asymmetric divisions generating neurons for different layers of the forming CP: SP first, then deep layers (L6, L5) and upper layers (L4, L3 and L2). The migration of neurons is realized in an inside-out fashion with newborn neurons migrating through layers of older neurons. In the same time, some of the cells from NPs divisions form intermediate progenitor cells (IPCs), migrating to the SVZ where they divide symmetrically contributing to the upper layer neurons. Around E17.5, gliogenesis starts by NPs generating astrocytes (Ast) in the cortex and subependymal zone (SEZ) and also forming a new layer of ependymal cells (EL). BV, blood vessel; CR, Cajal-Retzius cell; DL Pyr, deep-layer pyramidal neuron; IZ, intermediate zone; UL Pyr, upper-layer pyramidal neuron; WM, white matter.

1.1.1 Regulation of cortical layer formation

Birth-dating experiments conducted in mice and monkeys showed a specific order of neuron appearance in different cortical layers [19,20] and thereby demonstrated the spatio-temporal dependence of cortical layer formation [21,22]. The process of generating the six cortical layers composed of specific subtypes of differentiated neurons, astrocytes, and oligodendrocytes is regulated by a combination of extrinsic and intrinsic factors, such as growth factors and gene expression regulation pathways [18].

The initially formed preplate constitute mainly of Cajal-Retzius (CR) cells which play an important role in lamination of the cerebral cortex [23]. The next step in corticogenesis is the switch from CR cells to layer V-VI neurons, achieved by the suppression of CR cell fate and redirection towards DL neuron identity. Further neocortical neuron specification requires cross-regulatory determination of layer-specific subtype of cells through cell-specific transcription factors [24].

For DL neurons, factors such as SOX5, TBR1, and CTIP2 play a key role in differentiation and cell migration [13,14]. For example, in this interplay between transcription factors, SOX5 represses *Ctip2* expression in layer VI refining its layer V enriched pattern [13]. This repression is regulated further by TBR1 which promotes the identity of corticothalamic neurons occupying layer VI [25].

Different transcriptional programs control late-born neurons residing in UL. The transition from generating DL to more superficial-layer neurons requires the negative feedback of post-mitotic DL neurons themselves [26]. UL neuron identity is controlled by factors such as SATB2 or BRN1/2 among others [18,28,32].

At the late stage of corticogenesis, regulatory cascades are gradually restricting the neurogenic potential of progenitor cells shifting it towards gliogenesis. Before this happens, however, basic helix-loop-helix (bHLH) genes, such as *Mash1* or *Ngn2* repress astrocyte fate [29].

1.2 CELLULAR MICROENVIRONMENT

From the very beginning of embryonic development, all cells exist in a bigger context of the microenvironment. This microenvironment will have a great impact on the cell throughout its lifecycle leading to different outcomes even in genetically identical cell clones. The idea of environment shaping the cell fate is more than 200 years old [34]; however, it was proven almost a hundred years later by demonstrating that cells upon implantation in different regions of embryos, take different paths in their later development [35,36].

The microenvironment is a capacious term that can contain all the factors that directly or indirectly influence cells in a given space through physical, mechanical or biochemical interactions. The most commonly named factors are: the extracellular matrix (ECM), neighboring cells, mechanical forces, cytokines, hormones, growth factors, nutrients and oxygen levels. The totality of these factors, especially in the context of stem cells residing in them, is called the stem cell niche. Together, these components contribute to cell maintenance, migration, and differentiation [37–40] (Figure 2.).

The cellular environment plays a crucial role in every stage of cell life. Starting from development, where secreted growth factors affect epigenetic regulation of cells resulting in different developmental fates [41]. At later stages, the environment can regulate self-renewal, apoptosis and differentiation of stem cells within the adult stem cell niche influencing tissue maintenance and homeostasis [37]. Finally, the microenvironment can undergo changes in pathogenesis and is involved in cancer formation and progression [42].

In developmental biology, tissue engineering and cancer research, it is essential to consider the microenvironment and its influence on the system of interest, whether trying to understand its influence *in vivo* or recreating it *in vitro* for better modeling or regenerative medicine applications.

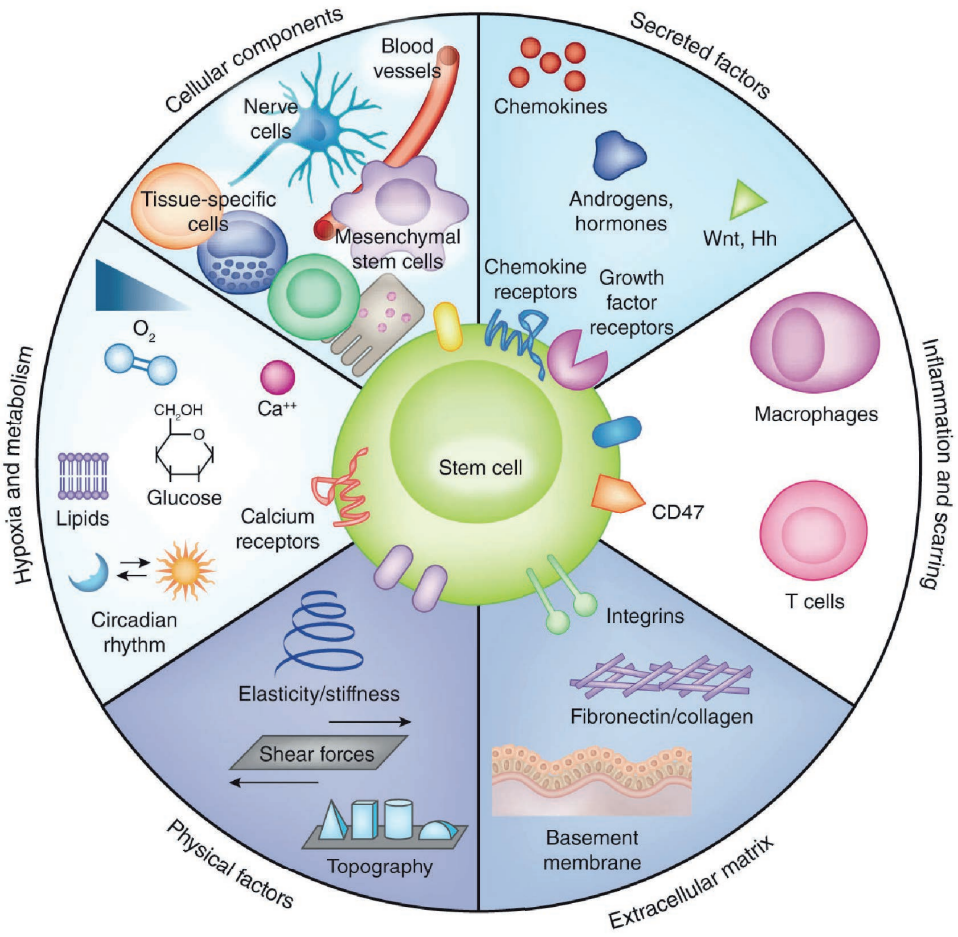

Figure 2. **Stem cell niche and the microenvironment influencing cells in the body**. The microenvironment surrounding cells is complex and dynamic: influencing cell behaviour but it is also modified by the cells. Reproduced from Lane et al. (2014) with permission from Springer Nature.

1.2.1 The ECM

The ECM is a complex network of proteins, proteoglycans and glycosaminoglycans (GAGs), creating a three-dimensional scaffold for cells and comprising an essential part of their microenvironment. The ECM is in a constant dynamic interaction with cells, influencing tissue development and homeostasis. Further, the ECM has several functions such as being a substrate for cell attachment organizing cells in three-dimensional space and in relation to each other as well as facilitating the transmission of signals and providing mechanical cues to modify cell behavior [43–45].

The cross-talk between cells and the ECM was described in the dynamic reciprocity model, which postulates that the ECM both modifies cell behavior but is also modified by cells over time [46]. In general, this bi-directional interplay is realized through membrane receptors such as integrins and/or mechanosensitive ion channels through a process called mechanotransduction [47]. The ECM's unique chemical and spatial composition will create different biochemical and biophysical environments suitable for different cell types i.e. providing attachment through cell-specific receptors and providing mechanical stimulation.

1.2.1.1 ECM stiffness

Every tissue can be characterized by specific mechanical properties which will result in different cellular responses, crucial during organ development but also its homeostasis in adult life. The human body displays a broad range of different elasticities that can be characterized by Young's modulus (E). The brain is one of the softest tissues in our body ($E \leq 4 \cdot 10^2$ Pa) while the muscle is in the middle of the spectrum ($E \geq 10^4$ Pa), bone closes the range, being the stiffest ($E \geq 10^9$ Pa) [48].

ECM stiffness has a great impact on several aspects of cellular behavior such as growth, survival, motility and differentiation. These responses are cell type-dependent and can have a different impact at different developmental stages. For example, mesenchymal stem cell (MSC) lineage specification can be altered depending on the substrate stiffness on which they are grown. Soft matrix, corresponding to brain stiffness, will result in neural differentiation, whereas a bone-like rigid environment will direct these cells into an osteogenic pathway, with myogenic differentiation on the intermediate substrates [38].

During mouse cortical development, tissue in all the layers undergoes significant changes in stiffness [49]. It was also shown, that NSCs similarly to MSCs can sense elasticity of the surrounding environment and respond to it with altered differentiation programs. Teixeira et al have shown that substrates resembling brain stiffness promote neuronal maturation of NSCs and increase astrocytic differentiation *in vitro* [44]; however, this response is likely to be stage dependent, as adult NSCs were found to generate more neurons and less glia cells in similar conditions [50].

1.2.1.2 Geometry of the ECM

The geometry of a cell's environment is another crucial parameter contributing to the cell niche. Cells are exposed to a dynamically changing three-dimensional (3D) world from the very beginning. During embryonic development monolayers of cells start to change their shape, transforming into early morphologies of different tissues and organs.

The spatial organization of the ECM can be viewed at different scales, from nano- to microarchitecture. It has been shown that the nanostructure of the cellular microenvironment can have a great impact on cells. Different geometries have been shown to drive MSCs into various differentiation programs. When cultured on rectangular or pentagonal shaped areas, MSCs displayed different outcomes, favouring either osteo- or adipogenic pathways depending on the growth conditions. This response is mediated through differential myosin contractility and subsequent gene expression alterations in the MAP kinase pathway and Wnt signaling [51]. MSCs neuronal differentiation can also be altered by geometry itself. It has been shown that a higher level of nanopattern complexity (spikiness) can stimulate MSCs to produce higher percentages of MAP2 positive cells [52]. The substrate topography is an important factor influencing also other cell types. It has been shown for instance that in NSCs nano-roughness of the surface on which they were cultured through the mechanosensing

cation channel Piezo-1, induced neurogenesis, despite the conditions normally favoring gliogenesis, suggesting the importance of the topography for NSCs differentation [53].

3D context at the microscale introduces different mechanics, cell-cell/cell-matrix interactions as well as oxygen and nutrient diffusion [54]. The 3D nature of the environment itself is enough to affect cellular morphology [55] and responses. Cell attachment, proliferation and migration can be enhanced when given a third dimension, compared to 2D conditions on the ECM with the exact same composition [56].

1.2.1.3 Attachment

Another role of the ECM is providing attachment for cells through specific interactions between cell membrane receptors and protein sequences in the ECM. There are two most common proteins providing adhesion: laminin and fibronectin.

Laminins exist in at least 16 different isoforms composed of α, β, and γ chains in different configurations. Its diverse forms can mediate cell attachment and cell functions such as differentiation or migration [57]. Cell attachment to laminin happens through integrin receptors and laminin G-like domains (LG) in the C-terminal region of the long laminin arm [58]. In the context of NSCs, laminins were shown to play an important role in promoting proliferation [59,60] and differentiation [61].

Another integrin-related cell-ECM binding is realized through one of the most studied adhesive peptides: arginine-glycine-aspartate (RGD). This tri-amino acid motif is present in many ECM proteins such as the aforementioned fibronectin, but also vitronectin or fibrinogen. Many different cell types use this mode of adhesion and this fact is widely used for engineering materials that are designed to promote cell attachment [62]. For instance, vitronectin derived sequence was used to functionalise recombinant spider silk used in Paper IV in this thesis.

1.2.2 Oxygen

Stem cells also respond to the metabolic status of the tissue that they reside in. One of the most important components of the niche microenvironment is oxygen. In adult tissues, the physiological oxygen concentration is estimated to be between 2-9% [63] which constitutes a, so-called, normoxic condition, much lower than atmospheric levels. However, during development, oxygen concentration on average can be even lower (approximiately 3%) due to the ongoing vascularization [64]. Human stem cells exposed to reduced oxygen levels (approximately 5%) in culture show increased proliferation [65].

Cells react to hypoxia mainly through hypoxia-inducible factor (HIF) family proteins. The HIF complex is composed of two subunits: HIF1α and HIF1β [66]. Under normoxic conditions, HIF1α is transported to the cytoplasm where it is proteolytically degraded [67]. Below 9% oxygen, HIF1α stabilizes and can dimerize with HIF1β. Upon translocation to the nucleus, it can transcriptionally activate genes involved in cell cycle regulation, angiogenesis

or glucose metabolism [68]. In the context of NSCs, hypoxia (1% oxygen) reduced cell differentiation into neurons upon FGF withdrawal through a Notch-mediated mechanism and its interaction with HIF1 [69]. It was also shown that HIF1α activation and interaction with the Notch signaling pathway in low oxygen environment can increase NSCs differentiation into astrocytes [70].

While creating relevant *in vitro* microenvironments, not only global oxygen concentration is important, but also local effects should be considered, especially in the context of 3D constructs. Oxygen availability for cells in such scenario depends mainly on the oxygen partial pressure and diffusion rates through the biomaterial. Further from the outer edge of a 3D construct oxygen levels can drop to suboptimal levels creating a hypoxic core [71,72].

1.2.3 CtBP2

Another mechanism of how cells respond to their microenvironment is through the redox sensing transcription corepressors CtBP, which has two similar homologs (CtBP1 and CtBP2) in vertebrates.

The center of the CtBP2 protein consists of a dimerization domain and a PLDLS-binding sequence which allows interactions with transcription factors. The N-terminal region in CtBP2 is different from that in CtBP1, as it contains a nuclear localization signal. These corepressor proteins have the unique property of sensing metabolic status by binding to both nicotinamide adenine dinucleotide (NAD+) and its reduced form NAD(H), but with higher affinity to the latter one, which is important for CtBP's enzymatic activity [73,74]. Moreover, dinucleotide binding promotes interactions between CtBP1 and CtBP2 to form homo- and hetero-dimers [73], which in turn can stimulate binding to some of the CtBP target proteins [75]. It has also been shown that higher nuclear levels of NAD(H) induced by chemical hypoxia, resulted in enhanced transcriptional repression by CtBP [76]. Recent evidence confirms the ability of CtBP1 and CtBP2 to form tetramers, also regulated by NAD(H) binding; however the exact physiological role of such a complex remains to be elucidated [77].

CtBP2 mutant mouse embryos show aberrant neural development with delayed forebrain and midbrain formation. *CtBP2*-null mice embryos eventually die by E10.5, whereas *CtBP1*-null mice show a less severe outcome resulting in smaller but viable animals upon birth, that die earlier than wild type mice. When both proteins were knocked out, the obtained phenotype was the most severe with embryos not even reaching the head fold stage [78].

The CtBP protein family is involved in oncogenesis and development controlling cell survival, proliferation and migration through binding to other transcription factors (over 30 identified by now) and interactions with histone deacetylases (HDAC1, HDAC2), demethylases (LSD1) and histone methyltransferases (HMTs) [78,79]. Moreover, CtBPs can act as co-repressors by the recruitment of Polycomb proteins to DNA and interactions with proteins such as p300 to repress their histone acetyltransferase function [80,81].

Both CtBP1 and 2 are linked to the suppression of apoptosis and the epithelial-mesenchymal transition (EMT) playing an important role in hypoxia-regulated E-cadherin suppression [82]. In addition, CtBP was found to be upregulated in different cancer cell types often linked with poor patient prognosis [83,84].

In the context of neuronal development, CtBP1 was shown to repress neuronal differentiation in the metabolic context of high levels of oxygen and bone morphogenic protein (BMP) in chick spinal cord by interaction with HES1 in a co-repression complex [85]. CtBP1 also interacts with the transcriptional repressor Ikaros [86] which in turn regulates the temporal identity of neurons in the mouse cortex during development [87]. Additionally, CtBP2 was found to interact with Zinc-finger E-box binding homebox 1 (ZEB1) in the mouse developing cortex [88]. ZEB1 is an important factor in the EMT involved in physiological and pathological processes such as neural crest formation or metastasis of carcinoma cells [42,89]. Overexpression of *Zeb1* in mouse embryonic brain at E14.5 was found to block progression from basal radial glial cells to neurons and disrupt normal cell migration in the developing cortex. Overexpression of *Ctbp2* in developing mouse brain in the same study resulted in higher percentage of immature IPs in IZ/SVZ and altered morphology of neurons [88]. However, there is no clear mechanism of how CtBP2 can influence neural stem cells, especially in the microenvironment perspective.

1.2.4 Microenvironment in pathology

The correct tissue microenvironment is both an indicator of and a required factor for organ homeostasis. However, it can undergo changes due to pathological processes, that will disrupt the balance that may promote disease progression and hamper potential treatment. The microenvironment in tumor development for example undergoes radical changes, such as remodeling of the ECM resulting in changes in mechanical properties. The stiffening of the matrix is a very common hallmark of developing tumors which was used for cancer diagnosis already in ancient times. The local architecture also undergoes modifications during tumor development: normally relaxed and randomly oriented collagen fibrils start to become thicker and aligned, which contributes to later metastasis [48,90].

1.3 NEUROBLASTOMA

Neuroblastoma (NB) is the most common (12-15% of all childhood cancers) and deadliest extracranial tumor in children. It originates in the sympathetic nervous system and is most likely derived from sympathoadrenal progenitor cells of the neural crest. NB is a highly heterogeneous malignancy and can be manifested in mild or severe forms, with very different prognoses: from up to 90% survival rates in patients diagnosed with low-risk types, down to only 50% in the high-risk groups. The high-risk and poor-outcome associated groups are often characterized by amplification of the developmental transcription factor and oncogene *MYCN*. The majority of patients demonstrate aggressive subtypes of NB, for which current therapies often fail. A part of the problem is a lack of successful pre-clinical models to study NB biology and the subsequent drug response [91].

In terms of its microenvironment, NB specimens from high-risk patients were found to be highly fibrous with collagen I as the main ECM component [92]. Moreover, NB cells *in vitro* displayed sensitivity to the microenvironment showing different morphology and gene expression in response to geometry and mechanical properties of the culture matrix [93,94].

1.4 RECREATING STEM CELL NICHE BY 3D BIOPRINTING

The idea of growing cells outside the human body was first introduced by Loeb in 1897 [95]. Since then, *in vitro* cell culture went a long way from just an idea to advanced technology. Establishing stem cell lines in 1998 [96] greatly contributed to the foundations of the tissue engineering field, which emerged as a "bridge" connecting research focused on whole organs and studies on culturing homogenous cells [97]. This combination of biology and engineering addresses critical problems in the treatment of tissue loss or organ failure. In spite of invaluable help in saving or improving countless lives, treatment based on transplantation of organs suffers from severe limitations such as donor shortage or immunological rejection [98]. Apart from application in therapeutics, tissue engineering can also be used in basic research to develop biomimetic *in vitro* tissues and organs to study physiology, toxicology, pathology of their natural equivalents as well as for drug testing [99–102].

To culture stem cells *in vitro,* optimal conditions should be provided to mimic their natural microenvironment. Numerous attempts were made to imitate the stem cell niche by using matrix components of different stiffness, modifying cell-cell mechanical interactions, manufacturing nanofibrous materials or introducing three-dimensionality into cell culture [38,103,104].

Conventional tissue engineering is based on manufacturing scaffolds and populating them homogenously with cells. This approach was successfully used for the generation of various tissues for clinical applications [105,106]. However, there are some limitations to traditional tissue engineering. One problem is the precision of controlling microarchitecture aspects of tissue constructs such as pore size, geometry and distribution or precise spatial location of cells [107,108]. Since localization of cells in tissue is crucial for proper organ formation and function [109] this requirement must be fulfilled for biological constructs that aim to reflect the *in vivo* situation.

To address this need, techniques such as photolithography, soft lithography, and stamping can be applied for microfabrication. However, they are not free from challenges such as limited range of compatible materials, low speed or method complexity [110]. Another approach to creating biomimetic tissues or organs is to utilize cell self-organization properties to create organoids [111]. However, some of the organoid-based models suffer from poor reproducibility and challenges in size and geometry control [112]. Some of these limitations can be solved with the bioprinting approach.

Bioprinting can be defined as a technology that allows the transfer of non-living materials such as proteins, drugs, biomaterials, ECM components and living cells to solid, gel, or liquid media with prescribed and precise spatial locations [113]. The very first reports of two-

dimensional bioprinting started to appear at the end of the 1980's [114] when a modified office inkjet printer was used to deposit cell adhesion proteins in predefined positions onto substrates. In 2003, this technology was used by Wilson and Boland to print viable cells for the first time [115]. But researchers did not stop only at 2D patterning. Adding the next dimension to printing was made possible thanks to the advancement in 3D manufacturing initiated by Charles W. Hull who invented a method called stereolithography in 1986. This technique was described as the generation of three-dimensional objects by additive application of fluid material that was cured by UV light in a layer-by-layer fashion [116]. In 2004, Smith et al first applied cell extrusion based on a similar principle for 3D deposition of viable cells [117].

Systems for extrusion-based printing usually have two main components: a dispensing system and a stage (Figure 3.). Dispensing systems are typically based on pneumatic pressure [118,119] or mechanical extrusion [120]. To allow material deposition in a predefined spatial pattern one or both components can move along the x, y and z-axis, controlled by computer software [121,122]. Materials are extruded continuously through the nozzle in the form of filament to create 2D or 3D constructs. During this process, one layer at a time can be deposited. Usually, in bioprinters, different hydrogels are used for extrusion. For that, the specific used hydrogel used must be able to flow through the nozzle in particular conditions. When the first layer is deposited, it can be cross-linked, thereafter another layer can be printed on top of it [123]. Depending on the used material, hydrogels can be cross-linked either physically (i.e. thermal or ionic crosslinking) or chemically [117,124,125]. Usually, high viscosity hydrogels are used – either with cells embedded (also called bioink) [126,127] or without cells [128–130].

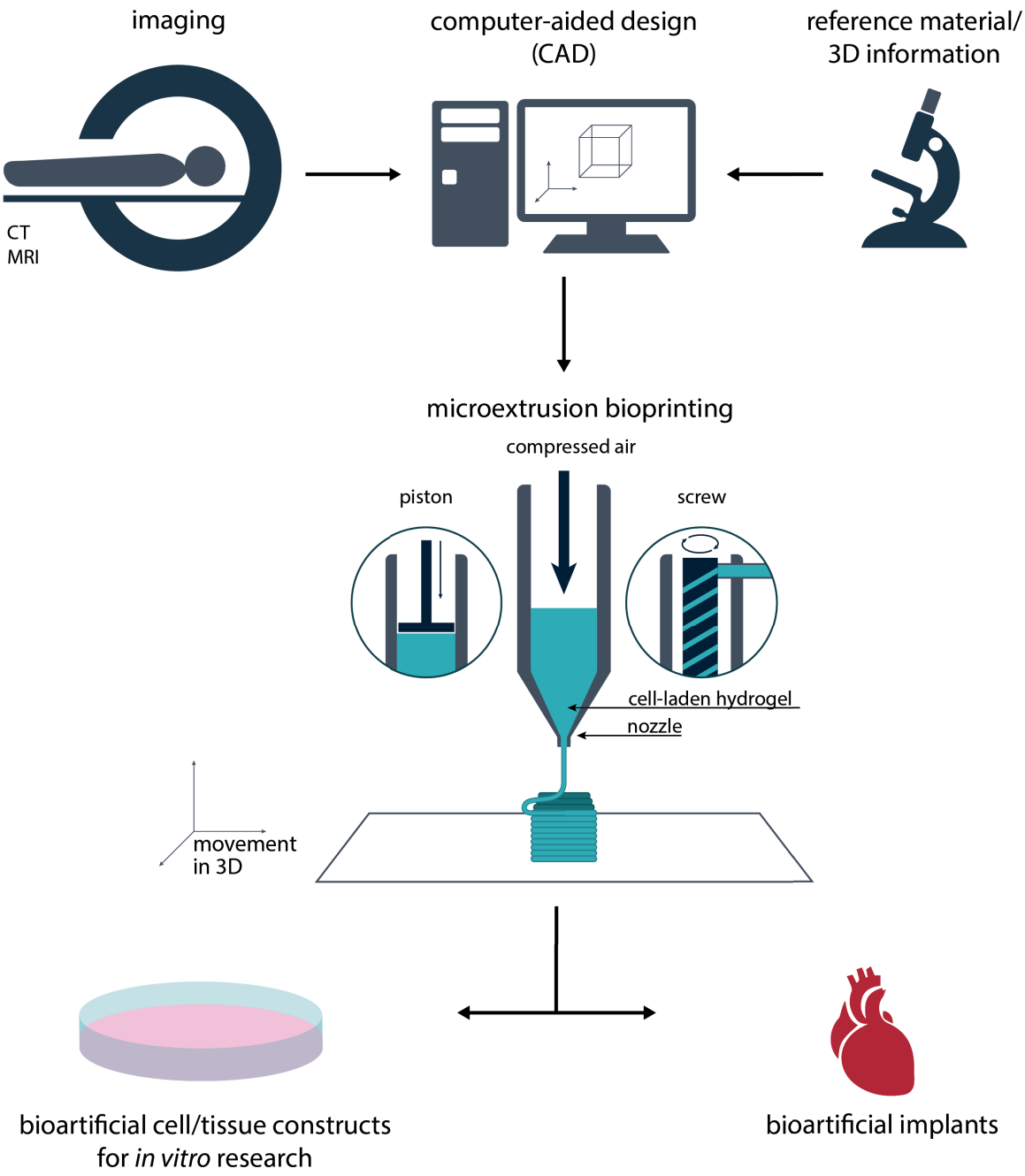

Figure 3. **Microextrusion 3D bioprinting workflow overview.** The 3D model is prepared using computer software and can be based on existing data from i.e. MRI patient scan. The 3D model is then translated into instructions for the 3D printer to follow. Microextrusion printing can be realized through different modalities: piston, pneumatic or screw driven. Cells mixed with hydrogel are deposited onto the printing platform in a layer-by-layer fashion. Such constructs can be later used for *in vitro* cell culture or implants for *in vivo* applications.

However, extrusion-based bioprinting is not restricted to hydrogels. Some methods utilize biocompatible thermoplastic polymers for stiffer scaffold manufacturing [131] or apply multicellular spheroids as bioink for tissue self-assembly [132]. The multitude of the parameters involved in extrusion-based 3D bioprinting, such as 3D model processing, biomaterials, cell density, extrusion pressure, printing speed, temperature, cross-linking, post-processing, and cell culture conditions must be orchestrated to achieve optimal results in terms of cell viability and print quality.

1.4.1 3D bioprinted *in vitro* tissues

3D bioprinting can recapitulate many aspects of the cellular microenvironment found *in vivo* for more accurate tissue modeling. With precise spatial control, bioprinters can construct geometries reassembling the microarchitecture of particular organs, including channels to mimic vascularization. Depending on the biomaterial used in the manufacturing process, properties such as stiffness, porosity, availability of cell-adhesion sites, and presence of extrinsic signals such as growth factors can be mimicked to reflect native tissue [133].

So far, bioprinting has successfully been employed to create promising 3D models of many physiological tissues, such as skin, bone, cardiac tissue and liver [134–137]. However, the potential of bioprinting is not only limited to mimicking healthy tissues. This technology is also becoming more popular for the creation of biological systems that aim at recreating a disease microenvironment. As in healthy tissue, the complexity of the tumor microenvironment is rarely mimicked by simplistic 2D *in vitro* models failing to test drug efficacy [138,139]. 3D bioprinted models of glioblastoma, mammary carcinoma, lung carcinoma, and many others were created, showing sensitivity to chemotherapeutics, drug distribution dynamics or metastasis behavior closer to the *in vivo* environment [140–142]. This opens possibilities for better preclinical models and precision medicine.

1.4.2 Biomaterials for bioprinting

Optimal biomaterials for 3D bioprinting remain a major challenge in the field. In general, they can be divided into two groups: naturally derived and synthetic. Some of the most popular materials belonging to the first group are alginate, collagen, chitosan, gelatin, and hyaluronic acid. Because of their natural origin, they provide many chemical signals for cells, enabling their attachment and growth. Nevertheless, naturally derived biomaterials often suffer from batch-to-batch variation and variable printability, which makes them difficult to apply to stem cell constructs, especially in a clinical context [143–146]. On the other hand, synthetic polymers such as poly(ethylene glycol) can provide better physical properties; however, they usually lack active binding sites, which results in low cell viability [147,148].

1.4.2.1 Sodium alginate

Sodium alginate (SA) is a sodium salt of alginate, a polymer naturally present in cell walls of brown algae (*Phaeophyceae*), which is its main commercial source; however, alginate can be also synthetized in bacteria. Alginates are a group of polymers which consist of L-guluronate (G) and D-mannuronate (M) residues arranged in blocks. These blocks can be only G, only M or combination of both in a sequence [149] (Figure 4.). The content, length and ratio of different blocks in alginate have an impact on the polymer mechanical properties. Usually, the longer the G-block and the higher the molecular weight, the better the mechanical properties of the resulting hydrogel. It is a consequence of the fact that only G-blocks of alginate are participating in alginate ionic crosslinking. This happens through the addition of divalent cations, such as Ca^{2+}, which are coordinated by guluronate blocks that

form junctions with each other to form a gel [150]. Ionic cross-linking using calcium chloride ($CaCl_2$) is the most common way of creating alginate-based hydrogels, however covalent, cell and thermal cross-linking are alternative options.

Biocompatibility, low toxicity and immunogenicity, cell-friendly cross-linking and low cost make SA a very versatile biomaterial. It found applications in wound healing, drug delivery and cell encapsulation for tissue engineering or cell transplantation [149]. Since the 1980s, when the first pancreatic islet cells were encapsulated in SA [151], this biomaterial was used for applications with many different cell types, such as MSCs, hepatocytes or myoblasts [152,153]. Immobilization of NB cells in SA microbeads was also reported [154]. It was shown that NB cells maintained their growth and electrophysiological activity while encapsulated in 3D SA hydrogel.

SA can also be used for 3D bioprinting, however, when low viscosity sodium alginate is used, it presents a challenge for precise material deposition with the maintenance of accurate 3D geometry. Methods such as coaxial nozzle-assisted 3D bioprinting can be used to overcome this problem, by extruding SA and $CaCl_2$ at the same time, causing rapid gelation [155]. However, applications of systems like this can be limited and an alternative might be needed. One of them is the freeform reversible embedding of suspended hydrogels (FRESH).

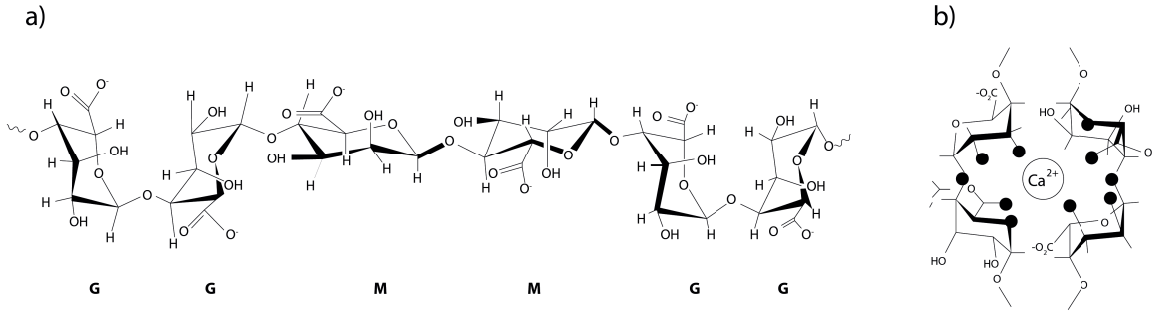

Figure 4. a) Molecular structure of sodium alginate. G, L-guluronate; M, D-mannuronate b) Interaction between the calcium ion and oxygen in gluronic acid.

FRESH is a bioprinting technique that allows for controlled deposition of hydrogels with low viscosity, providing support during the extrusion process as well as means for cross-linking of the printed material. Its main component is a support bath made of blended gelatin slurry, that has shear-thinning properties. The needle used for bioprinting, while immersed, can be freely moved around inside the slurry; however, when the SA is extruded, the support bath keeps it in place and start its gelation with a low concentration of $CaCl_2$. When the bioprinting process is done, gelatin can be dissolved in 37 °C and the 3D printed construct can be retrieved [156].

Despite being a versatile material, SA has its limitations. Hydrogel swelling, inadequate mechanical properties, lack of cell binding sites and printability challenges may reduce its application in some cases. Thus, alternative biomaterials should be considered.

1.4.2.2 Recombinant spider silk

One of the alternatives to naturally derived SA is synthetic, recombinant spider silk. Spider silk is one of the strongest materials naturally occurring in the environment. Its mechanical and biological properties were noticed and utilized already centuries ago for various applications: from fishing through garment production to medicine. Now, we understand the biochemical and mechanical properties of spider silk better than ever before and its characteristics remain attractive for medicine, especially for tissue engineering applications.

As spiders are territorial and it is difficult to farm them, numerous attempts were made to create a recombinant version to have access to larger quantities of the spider silk protein (spidroin) and control its composition. One of them was the production of a miniature spider silk protein 4RepCT in *E. coli*. Recombinant spider silks were found to be compatible with different cell type such as fibroblasts [157,158], bone marrow stromal cells [159], chondrocytes [160], human mesenchymal stem cells [161] and neural stem cells [162]. In addition to supporting cell growth *in vitro*, *in vivo* biocompatibility was also reported [163,164].

To better mimic the *in vivo* microenvironment recombinant spider silk was also applied in creating 3D constructs, however, these were sponges of random porous microarchitecture [162,165]. To overcome this limitation, 3D bioprinting was applied resulting in manufacturing cell-laden macroscopic constructs made of recombinant spider silk [166]. However, attempts to create artificial spider silk with mechanical properties similar to the natural equivalent remains a bottleneck in the field. This might be explained by the fact that denaturing conditions are usually applied for purification and fiber formation of recombinant spidroins [167]. Through the study of the natural process of dragline spinning, its mechanisms involved in it became clearer. Recently, the molecular basis of spider silk formation was better understood, highlighting the importance of carbonic anhydrase that creates a pH gradient in silk glands enabling proteins to polymerize [168]. Thus, it was suggested that the combination of recombinant spider silk with the right structure and low pH conditions, using an extrusion system (i.e. microfluidics device) could be a much better way of creating artificial spider silk [167]. A similar approach could be applied in a 3D bioprinting microextrusion system that additionally would give the advantage of spatially controlling the microarchitecture of the 3D construct.

Recently synthesized recombinant spider silk NT2RepCT that couples favorable mechanical properties with biomimetic spinning potential resulted in the toughest as-spun fibers thus far. The synthetic character of this spidroin allows for the introduction of additional cell attachment motifs such as RGD or IKVAV to better mimic the cellular microenvironment [159,169]. However, the exact cytocompatibility of the material and its effect on different cell types is not known yet. Thus, before fully realizing its potential, more studies have to be done.

2 AIMS OF THE THESIS

The general aim of this thesis was to investigate how microenvironment can affect and be translated to neural stem cells and what tools can be used to engineer microenvironment in *in vitro* cell culture.

The specific aims of the scientific papers included herein are to:

I. Investigate how the redox-sensitive CtBP2 protein influences cortical neurogenesis.
II. How different metabolic conditions affect CtBP2 acetylation and oligomerization status in rat neural stem cells *in vitro*.
III. Optimize the 3D bioprinting method to engineer a three-dimensional microenvironment for *in vitro* cell culture of human neuroblastoma cells.
IV. Assess the cytocompatibility of recombinant spider silk with human neural stem cells.

3 MATERIALS AND METHODS

3.1 ANIMALS

All animal experiments included in this thesis were conducted in compliance with the guidelines of the Swedish Board of Agriculture (ethical permits N284/11, N190/14 N329/11, N217/14) and were approved by the Karolinska Institutet Animal Care Committee.

3.2 *IN UTERO* ELECTROPORATION

In utero electroporation (Figure 5.) was performed as described elsewhere [170] with some modifications. Mouse embryos (E15) were injected with two siRNA constructs: control or *CtBP2* (Dharmacon/Accell), along with GFP plasmid at a 1:3 ratio and Fas Green into the lateral ventricle. The electroporation (CUY21 EDIT, TR Tech, Japan) used five 50V pulses at 50 ms with 950 ms breaks. Three days after electroporation, E18 embryos were recovered and sacrificed for brain collection.

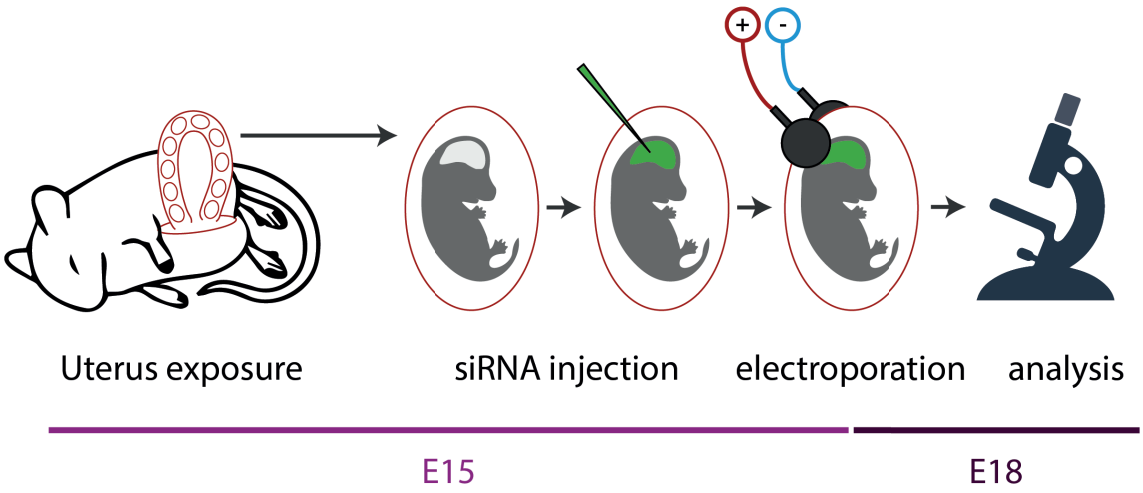

Figure 5. **Overview of the in utero electroporation.** At E15, the uterine horn is exposed during the surgery, mouse embryos are injected with siRNA constructs and GFP plasmid into the ventricle. Voltage is applied to deliver the construct to the cells. Mouse embryos are then sacrificed at E18 for sectioning, immunostaining and analysis.

3.3 BRAIN TISSUE PROCESSING AND CRYOSECTIONING

E18 mouse brains were fixed using 4% PFA for 2 days at 4 °C. Next, they were immersed in 30% sucrose solution for 4-7 days. Samples were mounted in TissueTek for cryostat sectioning at 18 µm slice thickness. Later, the slides were preserved at -80 °C.

3.4 FLUORESCENT LABELLING

3.4.1 Brain tissue immunostaining

Slides with E18 mouse cortex sections were rehydrated with 1X PBS for 5 minutes and subsequently permeabilized and blocked with 10% Normal Donkey Serum (NDS, Jackosn Immunoresearch) and 0.3% Triton x-100 in PBS for 1 hour at room temperature. Incubation

with primary antibodies (Table 1) at a 1:200 ratio was carried over-night at room temperature. Then, slides were washed 2x in PBS for 10 minutes. Incubations with secondary antibodies were carried for 1 hour at room temperature using 1:500 dilution. Next, samples were washed in PBS and incubated with DAPI/PBS solution (1:2000) for 1 minute, with subsequent washing in PBS for 2 minutes. Lastly, the slides were mounted using Vectashield medium.

Table 1**. Primary antibodies used for immunocyto-, histochemistry, and PLA.** RT, room temperature; ON, over night.

Antibody name	Host Species	Manufacturer and number	Concentration	Dilution	Temperature	Time
GFP	chicken	Aves (GFP-1010)	10 mg/ml	1:200	RT	ON
TUJ1	mouse	Biolegend (801202)	1.0 mg/ml	1:200	RT	ON
Nestin	goat	Neuromics (GT15114)	1.0 mg/ml	1:200	RT	ON
Ki67	rabbit	Abcam (ab15580)	1.0 mg/ml	1:200	RT	ON
PAX6	mouse	Covance (PRB-278P)	2.0 mg/ml	1:200	RT	ON
TBR2	rabbit	Abcam	0.7 mg/ml	1:200	RT	ON
CUX1	mouse	Abnova (521-620)	1.0 mg/ml	1:200	RT	ON
CTIP2	rat	Abcam (ab1846)	1.0 mg/ml	1:200	RT	ON
SATB2	mouse	Abcam	0.1 mg/ml	1:200	RT	ON
SOX9	goat	R&D Biosystems,(AF3075)	1.0 mg/ml	1:200	RT	ON
CtBP2 (immunohistochemistry)	rabbit	Abcam (ab96107)	0.33 mg/ml	1:200	RT	ON
CtBP2 (PLA)	rabbit	Abcam (ab128871)	0.5 mg/ml	1:200	37 °C	1h
CtBP2 (PLA)	mouse	BD Biosciences (612044)	0.25 mg/ml	1:200	37 °C	1h
SIRT1	rabbit	Santa Cruz (sc-15404)	0.2 mg/ml	1:50	37 °C	1h
pan-acetylated lysine	rabbit	Cell Signaling (9441)	1.0 mg/ml	1:200	37 °C	1h
p53	mouse	Cell Signaling (2524)	1.0 mg/ml	1:200	37 °C	1h
Vinculin	mouse	Sigma	N/A	1:100	37 °C	2h

3.4.2 Fluorescent staining of NESCs

NESCs were fixed using 4% PFA solution for 15 minutes at room temperature, then washed 2x in PBS for 5 minutes. Cells were permeabilized and blocked in 1% Bovine Serum Albumin (BSA, Sigma), 0.1% Triton x-100 for 30 minutes at room temperature.

Fixed samples were incubated with Alexa Fluor 488 Phalloidin (Thermo Fisher) diluted in PBS at 1:100 ratio for 1 hour at room temperature or primary antibody against vinculin (1:100 dilution in blocking solution) for 2h at room temperature (Table 1). Next, slides were washed 3x in PBS for 5 minutes. Samples incubated with anti-vinculin antibody were then incubated with secondary antibody (Alexa fluorophore 594, Thermo Fisher, 1:500 dilution in PBS) for 1 hour at room temperature. After that, samples were washed in PBS and mounted using a mounting medium with DAPI.

3.4.3 PLA

Proximity Ligation Assay (Figure 6.) kit (DuoLink/Sigma) was used on fixed and permeabilized NSCs using 4% PFA for 10 minutes and 0.1% Triton x-100 for 15 minutes. Next, samples were blocked using Blocking Solution (DuoLink) for 30 minutes at 37 °C. The primary antibodies used for PLA are described in Table 1. The overlapping C-terminal region was used for two different antibodies against CtBP2 for dimer detection. After the incubation, samples were washed 2x in Wash A solution included in the PLA kit, 5 minutes each. Next, detection probes were applied for 1 hour at 37 °C with subsequent 2x washing with Wash A. Ligation (30 minutes, 37 °C), 2x washing with Wash A, amplification (100 minutes, 37 °C), 2x washing with Wash B were carried in a sequence. For counterstaining, Alexa 488-Phalloidin (Molecular Probes) was applied. In the end, samples were mounted in DuoLink mounting medium.

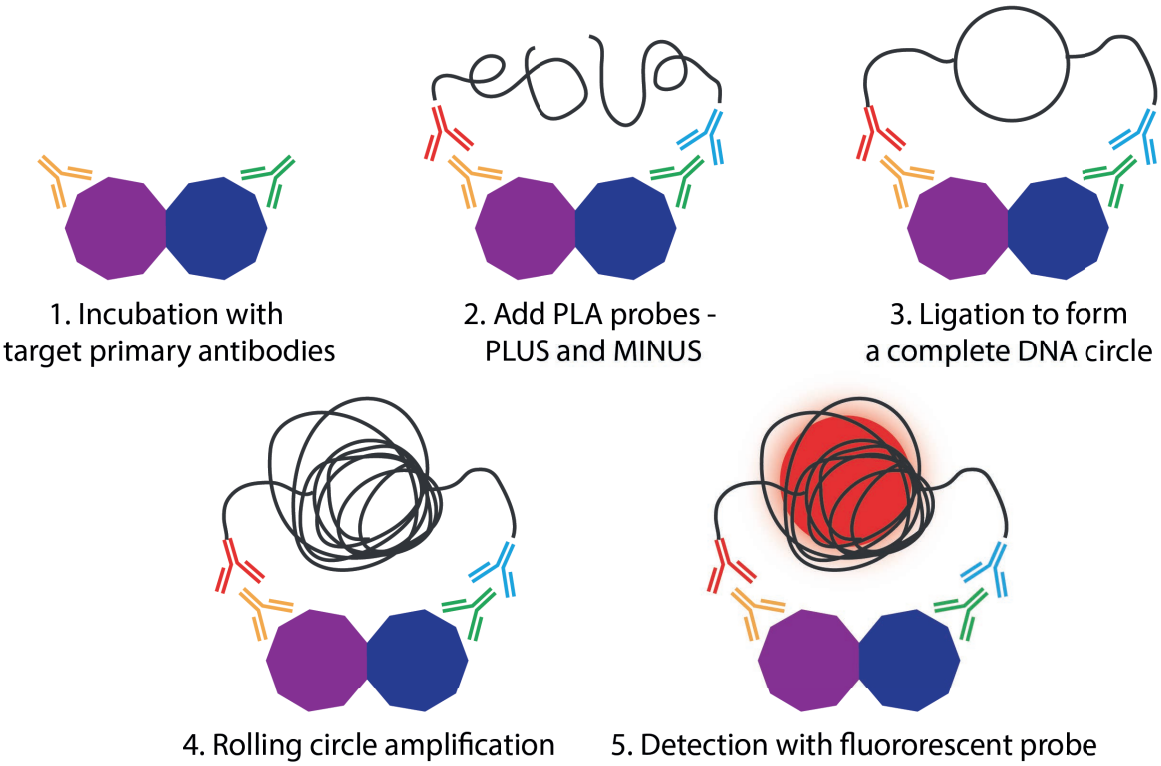

Figure 6. **Schematic overview of the PLA method principle.**

3.4.4 Viability assay

The live/dead assay (Life Technologies) for SKN-BE(2) cells was performed according to the manufacturer's instruction with minor modifications using 4 µM EtD and 2 µM calcein. For washing, DMEM/F12 media was used instead of PBS to prevent scaffold dissolution. For NESCs, 0.5 µM EtD and 0.2 µM calcein were used with a standard PBS washing.

3.4.5 EdU assay

The Click-iT EdU Alexa Fluor 594 kit (ThermoFisher) was used for detection of proliferating NESCs. 10 μM of EdU diluted in culture media was incubated with cells for 1 hour at 24 and 72h time points. Cells were then washed in PBS and fixed using 4% PFA for 15 minutes, followed by 3x washing 5 minutes each. The signal detection was carried out using EdU detection at room temperature for 30 minutes. Cell nuclei were stained using Hoechst. Samples were mounted in mounting media (Vectashield).

3.5 IMAGE ACQUISITION

The different samples were imaged with Zeiss LSM 700 confocal microscope, Operetta High Content Imaging system or Zeiss Observer Z1 inverted microscope and analyzed in ImageJ, Imaris or Harmony software.

3.6 CELL CULTURE

3.6.1 Rat NSCs

The developing cortex was isolated from E15.5 rat embryos and dissociated into single cells that were seeded in DMEM/F12 media supplemented with penicillin/streptomycin and modified N2 containing additional insulin. FGF2 (10 ng/ml) was added daily. Culture plates were coated using poly-l-ornithine and fibronectin solutions. Cells were cultured at 37 °C, 5% CO_2 and upon confluency, NSCs were split using HANKS solution. Only passage 1 and 2 were used for experiments.

For metabolic treatments, NSCs were either incubated in a hypoxia chamber (1% oxygen) or in normoxia with the addition of 5 mM 2DG (Sigma) overnight. Sirt1 inhibition was achieved using 1 mM Ex527 (Tocris). H_2O_2 treatment was conducted for 30 minutes or 1 hour using 500 μM solution.

3.6.2 SKN-BE(2)

SKN-BE(2) cells (ATCC, CRL-2271) NB cells were cultured at 37 °C, 5% CO_2 in DMEM/F12 culture media (Life Technologies) with 10% Fetal Bovine Serum (FBS, Sigma) and 0.1 mg/ml penicillin/streptomycin (Life Technologies). Every three days, culture media was replaced and when cells reached confluency, they were split using TrypLE (Life Technologies).

3.6.3 NESCs

Human iPSC derived neuroepithelial-like stem cells (NESCs) were maintained on plates coated with 20 mg/ml of poly-l-ornithine (Sigma) and 2 mg/ml of laminin (Sigma). Culture media consisted of DMEM/F12 with GlutaMAX (Gibco) supplemented with N2 (1:100, Gibco), 10 ng/ml rhFGF basic (R&D systems), 10 ng/mL rhEGF (R&D systems), B-27 supplement (1:1000, Gibco) and Penicillin/Streptomycin (Gibco). NESCs were passaged at 1:3 ratio every 2-3 days using TrypLE Express (Gibco) and trypsin inhibitor (Gibco). For

NESCs culture on spider silk or vitronectin coatings, cells were passaged at 4.375×10^4 cells/cm^2 to a P35 dish.

3.7 IMMUNOBLOTTING

The Bio-Rad Mini-Protean 3 system was used for immunoblotting. Electrophoresis and transfer performed according to the manufacturer's protocols. 30 mg of protein was loaded per well. The nitrocellulose membranes were blocked and later probed with LI–COR reagents. The Odyssey infra-red system was used for visualization. The following antibodies were used for western blot: CtBP2 (Abcam, 1:2000), SIRT1 (Santa Cruz, 1:100), Beta-actin (Sigma, 1:4000).

3.8 SIRNA-MEDIATED KNOCKDOWN

CtBP2 and *Sirt1* (Dharmacon) siRNA were delivered to NSCs by the Amaxa Nucleofection kit (Lonza). After nucleofection, NSCs were seeded in 35 mm plates in standard culturing conditions described above.

3.9 BIOMATERIALS

3.9.1 Sodium alginate

SA was prepared by dissolving 20 mg/ml SA (Allevi) in SK-N-BE(2) culture media. Additionally, for the POI experiments green fluorescent PLGA microspheres (Sigma) were added to SA at 4 mg/ml. For bioprinting with SKN-BE(2) cells, 2% SA was mixed with cells at $1 \cdot 10^7$/ml.

3.9.2 Recombinant spider silk

VN-NT2RepCT protein was produced as described before [13] with modification of introducing the VN motif: MGPNSPQVTRGDVFTLP. The VN-NT2RepCT construct was cloned using a pT7 plasmid in *E. coli.* Bacteria culture was carried overnight in Luria broth (LB) media with supplementation of kanamycin (70 mg/l) at 200 r.p.m shaking. 500 ml of LB media was then inoculated with culture from the previous step (1/100) and incubated at 30°C until reaching OD600 = 0.8. Then, to express the protein, the culture temperature was lowered to 20 °C and 0.3 mM isopropyl thiogalactoside was added. After overnight incubation, cells were collected by centrifugation at 5000 r.p.m. at 4 °C. Cell pellets were resuspended in 20 mM Tris buffer at pH = 8 and frozen at -20 °C, then lysed with a cell disrupter (T-S Series Machine, Constant Systems Limited) at 30 kPsi. Centrifuged lysate (30 minutes, 27000 g at 4°C) was loaded on a Ni-NTA column and protein was eluted with 300 mM imidazole. Protein extract was then dialyzed against 20 mM Tris buffer at 4 °C using a membrane with a molecular cut-off of 6-8 kDA. Finally, the product was concentrated using centrifugal filters (Vivaspin 20, GE Healthcare) at 4000g.

3.9.2.1 Cell culture plates coating

35 mm culture plates (Corning) were coated with VN-NT2RepCT, poly-l-ornithine/laminin and vitronectin. VN-NT2RepCT coating was achieved using two protein concentrations: 0.1 mg/ml and 1 mg/ml diluted in 20 mM HEPES/MES buffer (pH = 7.4), 20 mM TRIS buffer (pH = 8.15) and 2.5 mg/ml Glucono-delta-lactone (GDL). The coating was carried out over-night at 37 °C with subsequent plate sterilization using UV light. Control plates were coated using 20 mg/mL of poly-l-ornithine (Sigma) for 2 hours at 37 °C and second coating with 2 mg/mL of Laminin (Sigma) over-night at 37 °C. Vitronectin (Sigma) coating was carried out at 37 °C for 2 hours using 4.5 mg/ml of protein solution.

3.10 BIOPRINTING

3.10.1 FRESH preparation

40 mg/ml of gelatin was combined with 0.16 mg/ml of $CaCl_2$ and dissolved together in deionized water at 40 °C following an overnight incubation at 4 °C. A container with cooled gelatin was filled with a cold solution of 0.16 mg/ml $CaCl_2$ and blended in three 30-second pulses followed by 30-second breaks. The resulting gel was centrifuged for 2 minutes at 4000 RPM at 4 °C and after removal of the supernatant, gelatin was resuspended again in a cold 0.16 mg/ml $CaCl_2$ solution. Centrifugation and resuspension steps were repeated 3-4 times. Before printing, the slurry was spun down at 4 °C and 1100 RPM for 5 minutes and used for filling the printing container.

3.10.2 3D bioprinting

FRESH bioprinting (Figure 7.) was carried out using the Allevi 2 bioprinter (Allevi). 10 ml syringes (BD Biosciences) were filled with printing material and capped using a 2,54 cm long 30G blunt needle (Allevi). Four different pressures (5, 7.5, 10, 12.5 psi) and four different speeds (2, 4, 6, 8 mm/s) were used for extrusion of the material following gcode instructions. For FRESH slurry dissolution and crosslinking, 100 mM $CaCl_2$ solution was added to the printing container and incubated at 37 °C for 20 minutes. Next, dissolved gelatin was replaced with a fresh solution of $CaCl_2$ and incubation was continued for another 15 minutes.

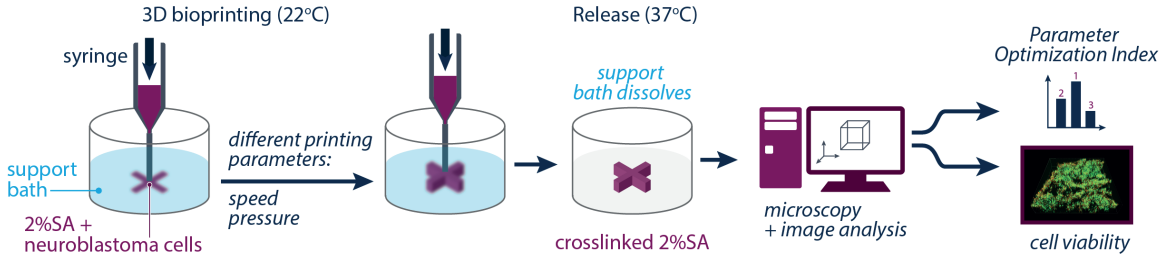

Figure 7. **Schematic overview of FRESH bioprinting and downstream analysis performed in Paper III.**

3.10.3 Determination of the Parameter Optimization Index (POI)

For SA visualization 4 mg/ml of green fluorescent PLGA microspheres (Sigma) were added to the printed hydrogel. Printed lines were imaged using Zeiss Observer Z1 inverted fluorescent microscope. Line width analysis was carried out using ImageJ software and custom-written script. POI calculations were done using formulas described elsewhere [171].

4 RESULTS & DISCUSSION

4.1 PAPER I

CtBP2 is an important co-repressor required for proper embryonic development. Double knock-out of *Ctbp2* in mice results in neuronal aberrations during development that result in embryos not surviving beyond embryonic day 10.5 (E) [78]. With previous insights from our laboratory into CtBPs role in the regulation of NSCs in spinal cord development [85], we decided to investigate the involvement of CtBP2 in cortex formation.

First, CtBP2 protein expression pattern was analyzed. It was previously shown that CtBP2 is expressed in both developing and adult brain [172,173], however we looked more closely into its colocalization with other markers at several different time points. We demonstrated that CtBP2 is widely expressed at all analyzed stages of embryonic development in the mouse brain, namely E13, E16 and E18. Immunocytochemistry exhibited CtBP2 protein localization in neural progenitor cells (Nestin positive) and neurons (Tuj1 positive) through all the layers of the developing cortex.

Upon successful knockdown of *Ctbp2* in E15 mice brains using siRNA and GFP vector delivered by *in utero* electroporation, we observed a different morphology of the analyzed brains 3 days later (E18).

Our first result indicated that in the *Ctbp2* knockdown group, cells that received *Ctbp2* siRNA together with GFP accumulated in the SVZ and IZ region. GFP+ cells in mice brains electroporated with control siRNA and GFP vector migrated to a large extent from SVZ/VZ to IZ and/or CP, demonstrating a more typical pattern of cell distribution. This accumulation of cells was a significant deviation compared to controls, with over twice as many GFP+ cells residing in the SVZ/VZ of the *Ctbp2* knockdown brains.

This result was further investigated by analysis of proliferating cells using Ki67 staining (a marker of the active phases of mitosis). Over 50% decrease of Ki67 GFP+ cells was found in the VZ/SVZ of *Ctbp2* knockdown brains, compared to controls. The difference in percentage of Ki67 GFP+ cells in other brain regions was not significant. These two results together, show that CtBP2 is important for NSCs proliferation, but also that it regulates the NSC migration to higher regions of the developing brain (IZ, CP). CtBP2 was previously reported to be involved in the regulation of proliferation in cancer cells [174,175], however our results link it also with neuronal development and proliferation of NSCs.

To understand the consequences of the *Ctbp2* knockdown in NSCs and its impact on neurogenesis, brain samples were immunostained for radial glia and intermediate neural precursor markers PAX6 and TBR2. Both populations of cells decreased by half in *Ctbp2* knockdown group when analyzed as a proportion of GFP+ cells. In the developing brain, PAX6 neural progenitors give rise to TBR2+ cells, that later differentiate into excitatory cortical neurons [176,177]. Disruption of this sequential pattern by *Ctbp2* knockdown suggest that it is important for maintenance of the NSC pool and proper differentiation. It

was previously presented that *Ctbp2* knockdown in a neural crest *in vitro* culture can lead to altered differentiation, with less neuronal cells and altered regulation of Wnt pathway related genes [178].

To validate this result, we also investigated the cellular composition of different cortical layers in the developing brain. Upon *Ctbp2* knockdown, the population of GFP+ upper layers neurons, characterized by SATB2 [179], decreased by one-third compared to control. Simultaneously, no CUX1+ cells, normally representative for upper cortical layers, were found in treated brains among the cells with *Ctbp2* knockdown. CtBP2 was previously shown to regulate cell migration in cancer cells [82,180] and since newborn neurons need to undergo migration for their maturation [181], disrupted cortical layer formation found by us suggests a role of CtBP2 also in migration regulation. This is further evident in recent studies of overexpression of *Ctbp2* in developing mouse brain that exhibit disrupted neuronal migration patterns with cells accumulating in IZ, strengthening our hypothesis [88].

CtBP2 is well known to be sensitive to the metabolic state of the surrounding microenvironment, through increased affinity to NAD(H), which is normally built up in hypoxic conditions [73,74]. Previous studies from our laboratory also suggest that CtBPs can integrate high oxygen and BMP levels to regulate NSCs state in the developing spinal cord. Moreover, it is being increasingly recognized, that oxygen levels and metabolism have an impact on NSCs and proper brain development [182]. This suggests, a possibility of CtBP2 involvement in metabolism sensing (for example different oxygen levels due to proximity of progenitor cells to blood vessels [183]) and translation to NSCs fate regulation.

4.2 PAPER II

This study took a closer look at CtBP2 function *in vitro* using NSCs derived from embryonic rat cortex. We focused on CtBP2 acetylation, an important aspect of its enzymatic activity and a factor influencing its dimerization. This acetylation is mediated by histone acetyltransferase (HAT) p300 [184]. Moreover, many proteins acetylated by p300 are deacetylated by SIRT1, an HDAC class III [185]. This fact is of even more importance knowing that SIRT1 can also, just like CtBP2, be regulated by NAD/NAD(H) ratio and was shown to suppress proliferation of neuronal progenitor cells shifting their differentiation towards the astroglial lineage [186].

Using a proximity ligation assay (PLA), we were able to show that CtBP2 and SIRT1 are found in close proximity in proliferating NSCs. PLA can detect protein-protein interactions if they are within 40 nm to each other [187], thus the signal detected can mean direct CtBP2-SIRT1 binding or presence in the same, bigger complex.

Since CtBP2 can respond to oxygen levels, and NAD(H) binding can influence its dimerization and activity, we looked at how different metabolic conditions can influence CtBP2 acetylation status in NSCs *in vitro*. One condition was a culture at 1% oxygen, a hypoxic environment which increased NAD(H) cellular levels. The second treatment was addition of 2-Deoxy-D-glucose (2DG), a glycolysis inhibitor, that turns down the

NAD(H)/NAD ratio. In both cases, CtBP2 acetylation levels increased by approximately 50%, as assessed with PLA, compared to control normoxic cell culture (21% oxygen). However, the interaction between CtBP2 and SIRT1 in different metabolic treatments did not change. Since it was previously shown that hypoxia and 2DG can alter SIRT1 activity [188], we speculated that acetylation changes in CtBP2 in different metabolic conditions could be an effect of interaction of these two proteins. However, treatment with Ex527, a SIRT1 inhibitor, did not change CtBP2 acetylation status, indicating that metabolic-dependent acetylation of CtBP2 is independent of SIRT1.

Following the investigation of how CtBP2 is influenced by metabolism, we checked homodimerization of CtBP2 under hypoxia and 2DG treatment. We observed decreased PLA signal for CtBP2 dimers in 1% oxygen environment in NSCs. This finding contrasts previous reports showing a positive correlation between NAD(H) levels and homodimerization of CtBP2 [189], however PLA result has to be viewed as a signal drop, that can effectively mean either decrease in homodimerization or shift towards higher level of oligomerization, such as formation of tetramers. In light of recent findings that CtBP2 can form tetramers in the presence of high NAD(H) levels, the latter option seems highly possible [77].

Results from paper I and II together show the importance of CtBP2 in the regulation of NSCs and the impact that metabolic conditions have on CtBP2. More investigation would be necessary to find direct links between CtBP2's role in translating oxygen levels into NSCs maintenance and differentiation in the developing cortex, however these results show CtBP2 as a potential candidate in this scenario. Paper II is also an important lesson, how an *in vitro* created microenvironment can influence molecular aspects of NSCs culture and it should be considered when correct stimulation is to be modeled.

4.3 PAPER III

Previous papers looked at the NSCs in their *in vivo* or *in vitro* environments. In paper III, the focus was on creating a microenvironment for human NB (SKN-BE(2)) 3D cell culture using the bioprinting technique. A substantial amount of evidence shows that cell culture in general and in particular cancer models can benefit from 3D modeling *in vitro*. Cell viability, proliferation, migration, gene expression, drug metabolism and many other aspects can often be mimicked better in 3D [190]. One approach to engineer such a microenvironment is by applying a 3D bioprinting technique. However, before printing a successful cancer model, which can reflect tumor biology accurately, several aspects of the manufacturing process should be optimized.

Printing NB cells in a soft matrix, such as 2% SA, may be beneficial for more *in vivo*-like gene expression [93]; however, it is a challenge on its own. To make it possible, we used a bioprinting technique with support material, called FRESH. To achieve the best printability and the lowest theoretical shear stress (TSS), that can be harmful to cells, a Parameter Optimization Index (POI) [171] assessment was performed for different printing speeds and extrusion pressures.

Our results confirmed that 2% SA is a suitable substrate for NB encapsulation. This biomaterial was previously reported to be compatible with murine NB cells [154,191], however we used a human cell line in our study, for a translational focus.

While printing 2% SA using the FRESH technique and a range of different parameters, such as speed (2, 4, 6, 8 mm/s) and pressure (5, 7.5, 10, 12.5 psi), we evaluated the width of the printed lines, to find the most optimal settings. This data was used to calculate a normalised POI value, which when closer to 1 reflects a better set of parameters. We compared POI for printing 2% SA alone or with a high concentration of SKN-BE(2) cells (10^6 cells/ml), and we observed significant differences in the printed line width while using the same extrusion conditions. This translated directly into 3D construct durability in the liquid media. It was previously shown, that cells encapsulated in a hydrogel precursor can affect its mechanical properties [192] and here we also presented how this factor influences the material printability.

The highest POI for printing 2% SA with SKN-BE(2) cells was achieved at 7.5 psi extrusion pressure and 8mm/s printing speed. Based on the original POI findings by Webb and Doyle, we expected this set of parameters to be optimal for printing the cells in terms of print quality and cell viability [171]. However, based on a live/dead assay, we observed that at 24h post-printing significantly more viable cells are found in prints exposed to higher pressure (12.5 psi, 52% viable cells) than in the 7.5 psi group (19% live cells). This finding was in contrast to our hypothesis, that lower POI with higher TSS will result in decreased cell viability. The negative impact of extrusion pressure on cell viability was previously reported [119,193]. The reverse correlation found by us could be contributed to the fact that we used low pressures (5-12.5 psi) for the extrusion, whereas other reports show impact on viability between larger pressure differences (i.e. 5 vs 20 psi). It is also possible that more cells extruded with higher pressure (keeping the same cell density) resulted in increased cell aggregation that had a protective role increasing overall viability [194]. When cultured for 7 days, SKN-BE(2) cells recovered from initially low viability (52% vs 83% of viable cells after 24h and 7d respectively).

The final observation is related to the 3D bioprinted construct integrity when using different printing parameters. The set of parameters from the highest POI for printing 2% SA with SKN-BE(2) cells resulted in constructs that dissolved easily during prolonged cell culture. Thin lines might be desired for fine detail printing, however they may compromise integrity of the final product. Inclusion of the cells in the hydrogel can impact the local microenvironment via proliferation, migration and ECM remodeling [195].

In conclusion, paper III shows successful 3D bioprinting of human NB cells using the FRESH technique and broadens the perspective of using quantitative printing optimization methods, such as POI, taking into consideration cellular loading of the hydrogels and long-term cell culture. Results of the paper III can extend beyond NB printing and be applied to creating microenvironments for other cell types, including NSCs.

4.4 PAPER IV

Sodium alginate used in Paper III was a sufficient biomaterial for NB cell culture, however, when superior mechanical properties or addition of cell binding motifs are needed, some alternatives might be preferable. Therefore, paper IV focuses on cytocompatibility of recombinant spider silk modified with vitronectin adhesion peptide, VN-NT2RepCT, with human iPSC-derived neuroepithelial-like stem cells (NESCs). This particular version of spider silk protein has an advantage of being xeno-free and a mechanically robust material that has the potential to be patterned in 3D using a process mimicking natural spider web weaving [196].

Initially, unmodified NT2RepCT protein was used for the culture of NESCs cells. However, we did not observe any cell attachment to the substrate. Since previous reports showed vitronectin addition to the recombinant spider silk as an effective modification enhancing attachment of human pluripotent stem cells [197], we applied that to the NT2RepCT protein tested here.

To asses vitronectin-modified spider silk (VN-NT2RepCT) performance as a substrate for NESCs culture, we compared it to the current standard double coating: poly-l-ornithine/laminin. Additionally, we used vitronectin alone as an additional control. Two concentrations of VN-NT2RepCT were used for culture plates coating: 0.1 and 1 mg/ml. The cells were grown for up to 72h and their viability, proliferation and cytoskeleton were studied.

NESCs grown in all of these conditions displayed high viability (over 90%) when assessed with live/dead assay. Similarly, proliferation rates confirmed with EdU staining were typical for NESCs and oscillated around 30% on all substrates. This confirmed that VN-NT2RepCT can support NESCs attachment, survival and proliferation for *in vitro* cell culture and that this biomaterial matches its performance with current standard coating: laminin.

When the cell morphology and cytoskeleton was examined in different culture environments, we observed a more stretched morphology of NESCs grown on spider silk and vitronectin coated plates. F-actin staining revealed more organized and elongated fibers on these substrates compared to laminin coating. Additional vinculin staining revealed a significantly higher percentage of cells with positive vinculin staining for vitronectin (77%), 0.1 mg/ml VN-NT2RepCT (84%), 1 mg/ml VN-NT2RepCT (88%) compared to laminin (35%). Moreover, vinculin morphology itself appeared to be more elongated for spider silk coatings in both concentrations than in pure vitronectin group, suggesting the presence of different forces involved in cellular attachment on different substrates. Vinculin is an actin-binding protein that is involved in FA formation, an important step in cell linkage to its substrate [198]. When its expression was abolished in mouse embryos, it led to brain development defects and embryonic lethality [199]. FA number and size were also found to be reduced in olfactory neurosphere-derived cells from schizophrenia patients, suggesting its implication in pathological processes [200]. Thus, differences in vinculin expression and morphology may have important significance in NESCs biology that should be investigated further.

Paper IV lays a foundation for the future application of VN-NT2RepCT in NESCs culture. Its mechanical properties and origin from the heterologous host (*Escherichia coli*) make this particular protein a very attractive candidate both for *in vitro* research but also for clinical applications. Moreover, NT2RepCT was designed to be able to recapitulate the natural spider silk spinning process using shear forces and low pH buffers and was shown to form fibers using a microfluidic device [196]. This property could be potentially exploited to use VN-NT2RepCT as a biomaterial for scaffold manufacturing using a 3D bioprinting process for NESCs culture to better mimic their natural microenvironment.

5 CONCLUSIONS

To paraphrase the English poet John Donne: “no cell is an island”. Naturally, cells do not exist in isolation from each other or the surrounding world. The cellular microcosmos is not a vacuum deprived of stimuli, it is quite the opposite: filled with neighbouring cells, biochemical factors and mechanical forces. Their influence is well recognized by now and it is a foundation to several fields such as mechanobiology or tissue engineering. However, we only start to understand the importance of the tissue microenvironment for physiology and pathology and our ability to model it *in vitro* is still in the early stage.

The work presented here, even though focuses on a small fragment of the big picture, it contributes to our understanding how the microenvironment may influence NSCs, what possible mechanisms are behind it and further looks into which tools can be applied to engineer the microenvironment for laboratory research.

We have shown the significance of CtBP2, a redox-sensing co-repressor protein in cortical neurodevelopment. By knocking it down in the developing mouse brain, we observed a defective phenotype suggesting a significant role that CtBP2 plays in NSCs differentiation and migration. An investigation of the protein itself revealed microenvironmental cues that regulate its post-translational modifications in neural stem cells *in vitro*. This gives us an important base for further studies to investigate if and how CtBP2 could translate the redox status of the cells to their regulation in the developing brain.

We have also validated and improved a 3D bioprinting optimization method suitable for the deposition of soft hydrogels and live cells. A 3D bioprinted model of NB showing good viability over prolonged cell culture can serve as a tool for more investigation in its biology, however our findings can be translated to other cell types as well. This opens up possibilities of co-printing NB with other relevant cell types (for example cells of the immune system) or other models of healthy tissues. Our approach may also be applied to other biomaterials. To initiate studies in this regard, we investigated the cytocompatibility of recombinant spider silk with NESCs cells. We have shown that this new recombinant protein supports growth and proliferation of human-derived neural stem cells. We have also gained insights into cell attachment to the substrate of interest, an important and interesting observation of different cytoskeletal arrangement that can potentially influence cell behavior. More studies will be necessary to investigate its functional aspect.

By showing the cytocompatibility of VN-NT2RepCT with NESCs, we confirmed the possibility of using this biomaterial for 2D cell culture, but our results also suggest a potential application of recombinant spider silk as a substrate for creating 3D scaffolds for modeling NESCs to a prescribed geometry.

No cell is an island, and as the oceans are the least explored environments on our planet, the sea of influences and archipelago of interdependencies in the cellular world remain to be conquered.

6 ACKNOWLEDGMENTS

Just as cells are not alone in our tissues, neither was I during my PhD. I was lucky to be in a great “microenvironment” of people that I would like to sincerely thank.

Ola Hermanson, my supervisor, for giving me the opportunity to join his lab. For trusting in me and giving me a lot of freedom for scientific and life explorations. For making our lab a creative space that was never boring. And for talks over a beer, about the beer and superheroes.

Part of Ola’s success is his radar for interesting people that he attracts to the lab. I would like to thank all previous and current members of the Hermanson pack. **Aileen** for being a good friend and my work wife and for our long venting sessions in your office. **Michalina** for giving me the comfort of familiarity when I just started my PhD (I guess same last name feels almost like a family ;)). **Esra** for being my teacher and friend. For our skateboarding sessions in the basement, your playlists that we listened to in the lab and countless hours of talking about everything. **Giulia** for your creative inspirations. **Xiaofei** for your scientific mind and a warm hart – both helped me many times. For teaching me Chinese and your Chinese tea and medicine when I was sick ;) **Moumita, Shirin, Bianca, Jose** and **Christina**, for a bit shorter, yet fun ride we had together on the train called PhD.

An important part of my PhD were the students I supervised during these years. **Liisi, André, Reinier, Ibra, Joost, Caoimhe, Anne.** You taught me how to be a better scientist and you were a great company in the lab, thank you!

Special thanks to all my KI friends that made coming to work a pleasure. **Alca** for being so warm-hearted and a good listener. Thanks for your Slavic spirit that always cheered me up. **Dagmara** for being purely awesome and the best snowboarding instructor. Your passions are my inspiration, thank you for that! **Konstantinos** for being a great and relaxed corridor-mate. **Joanne** for Dopper consultations and great wedding dancing moves. **Ania** for coffees on every possible floor in Biomedicum and cosplay stories. **Karen** for our lunches and being my plate-reader-mate. **Paola**, for going together through burning-man dust storms and showing me that Nutella goes well with Parmigiano. **Patrick** for the best IT/bartending/party support. You definitely added some life to our corridor. **Nicolas** for your hilarious sense of humor that I missed every day since you left KI. **Teresa**, for your passion for science communication and inspiring me with it. **Ben** for random comedy shows on your way for a coffee. **Molly** for making my trips to Hong Kong nice memories. **Elżbieta**, for our morning chats at the reception. KI is not the same place without you. You have brightened up my mornings.

I would also like to thank our collaborators and science-friends, that were there to discuss and support: **Anna Falk with her lab**, **Anna Rising**, **Ana Teixeira** and **Anna Herland**. I can see a pattern here!

My colleagues at Allevi: **Ricky**, **Maddie**, **Maggie**, **Taci** and **Gabe**. You have shown me another side of science and gave me an amazing start-up experience including crazy Thursday after-works. **Thom**, who was a part of my American experience and the best roommate I could imagine. Thanks for bike rides around Philly and making my stay in the US so memorable.

My true best friends: **Tomek** and **Michał**. I know that if I'm ever in trouble at the end of the world you will come armed and with a cold beer. **Tomek**, thank you for being there for me no matter the situation. For all the games we played, travels and evry nail hammered together. **Michał** for being a great friend, no matter the distance between us. Thanks for all the times you came to visit me and offered me a warmed-up Volvo seat. **Magda M.** for being my private trainer, taking me to my first rave and also breathing same dust on the Playa. **Kuba R.** for being a great gaming buddy and all the hours we spent on Golmud hills. **Tobias** for being my first friend in Stockholm, teaching me what a good Whiskey is and all the good times with the Loopin Loiue.

Madzia, thank you for supporting me in every aspect of my life. For your patience and energy that always keep me in balance. For all the amazing travels, we collected. And for every blueberry pancake we ate together.

My family: **Mama**, **Tata**, **Babcia** and **Marcin.** My most sincere thanks to my parents for all the effort they made to help me be in the place I wanted. For all their unconditional love and heavy packages with goodies from home. My grandma for preparing these goodies for me and making my every visit at home so warm. My brother for all the support and always having my back.

Mamuś, Tatuś, dziękuję Wam za to, że dzięki Wam jestem tu gdzie jestem i jestem tym kim jestem. Za Waszą miłość i wsparcie na każdym kroku. Babciu, dziękuję za to, że masz dla mnie specjalne miejsce w sercu.

7 REFERENCES

[1] N. Osumi, T. Kikkawa, Cortical Development, in: Cortical Dev. Neural Divers. Neocortical Organ., Springer Berlin Heidelberg, Berlin, Heidelberg, 2013: pp. 43–61. doi:10.1007/978-4-431-54496-8.

[2] R.L. Sidman, P. Rakic, Neuronal migration, with special reference to developing human brain: a review, Brain Res. 62 (1973) 1–35. doi:10.1016/0006-8993(73)90617-3.

[3] H. Wichterle, D.H. Turnbull, S. Nery, G. Fishell, A. Alvarez-Buylla, In utero fate mapping reveals distinct migratory pathways and fates of neurons born in the mammalian basal forebrain., Development. 128 (2001) 3759–3771.

[4] S.A. Anderson, Distinct Origins of Neocortical Projection Neurons and Interneurons In Vivo, Cereb. Cortex. 12 (2002) 702–709. doi:10.1093/cercor/12.7.702.

[5] S.C. Noctor, A.C. Flint, T.A. Weissman, R.S. Dammerman, A.R. Kriegstein, Neurons derived from radial glial cells establish radial units in neocortex, Nature. 409 (2001) 714–720. doi:Doi 10.1038/35055553.

[6] P. Rakic, A small step for the cell, a giant leap for mankind: a hypothesis of neocortical expansion during evolution, Trends Neurosci. 18 (1995) 383–388. doi:10.1016/0166-2236(95)93934-P.

[7] M. Götz, A. Stoykova, P. Gruss, Pax6 controls radial glia differentiation in the cerebral cortex, Neuron. 21 (1998) 1031–1044. doi:10.1016/S0896-6273(00)80621-2.

[8] T. Miyata, A. Kawaguchi, K. Saito, M. Kawano, T. Muto, M. Ogawa, Asymmetric production of surface-dividing and non-surface-dividing cortical progenitor cells, Development. 131 (2004) 3133. doi:10.1242/dev.01173.

[9] W. Haubensak, A. Attardo, W. Denk, W.B. Huttner, Neurons arise in the basal neuroepithelium of the early mammalian telencephalon: a major site of neurogenesis, Pnas. 101 (2004) 3196–3201. doi:10.1073/pnas.0308600100.

[10] M. Götz, Y.A. Barde, Radial glial cells: Defined and major intermediates between embryonicstem cells and CNS neurons, Neuron. 46 (2005) 369–372. doi:10.1016/j.neuron.2005.04.012.

[11] M. Nieto, E.S. Monuki, H. Tang, J. Imitola, N. Haubst, S.J. Khoury, J. Cunningham, M. Gotz, C.A. Walsh, Expression of Cux-1 and Cux-2 in the subventricular zone and upper layers II-IV of the cerebral cortex, J. Comp. Neurol. 479 (2004) 168–180. doi:10.1002/cne.20322.

[12] S.C. Noctor, V. Martínez-Cerdeño, L. Ivic, A.R. Kriegstein, Cortical neurons arise in symmetric and asymmetric division zones and migrate through specific phases., Nat. Neurosci. 7 (2004) 136–144. doi:10.1038/nn1172.

[13] K.Y. Kwan, M.M.S. Lam, Ž. Krsnik, Y.I. Kawasawa, V. Lefebvre, N. Šestan, SOX5 postmitotically regulates migration, postmigratory differentiation, and projections of subplate and deep-layer neocortical neurons, Proc. Natl. Acad. Sci. U. S. A. 105 (2008) 16021–16026. doi:10.1073/pnas.0806791105.

[14] P. Arlotta, B.J. Molyneaux, J. Chen, J. Inoue, R. Kominami, J.D. MacKlis, Neuronal subtype-specific genes that control corticospinal motor neuron development in vivo, Neuron. 45 (2005) 207–221. doi:10.1016/j.neuron.2004.12.036.

[15] R.F. Hevner, L. Shi, N. Justice, Y.P. Hsueh, M. Sheng, S. Smiga, A. Bulfone, A.M. Goffinet, A.T. Campagnoni, J.L.R. Rubenstein, Tbr1 regulates differentiation of the preplate and layer 6, Neuron. 29 (2001) 353–366. doi:10.1016/S0896-6273(01)00211-2.

[16] R.J. McEvilly, M. Ortiz de Diaz, M.D. Schonemann, F. Hooshmand, M.G. Rosenfeld, Transcriptional regulation of cortical neuron migration by POU domain factors, Science (80-.). 295 (2002) 1528–1532. doi:10.1126/science.1067132.

[17] K.Y. Kwan, N. Sestan, E.S. Anton, Transcriptional co-regulation of neuronal

migration and laminar identity in the neocortex, Development. 139 (2012) 1535–1546. doi:10.1242/dev.069963.
[18] H. Okano, S. Temple, Cell types to order: temporal specification of CNS stem cells, Curr. Opin. Neurobiol. 19 (2009) 112–119. doi:10.1016/j.conb.2009.04.003.
[19] J.B. Angevine, R.L. Sidman, Autoradiographic study of cell migration during histogenesis of cerebral cortex in the mouse., Nature. 192 (1961) 766–768. doi:10.1038/192766b0.
[20] P. Rakic, Neurons in Rhesus Monkey Visual Cortex: Systematic Relation between Time of Origin and Eventual Disposition, Science (80-.). 183 (1974) 425–427. doi:10.1126/science.183.4123.425.
[21] S.K. McConnell, Fates of visual cortical neurons in the ferret after isochronic and heterochronic transplantation., J. Neurosci. 8 (1988) 945–974.
[22] G.D. Frantz, S.K. McConnell, Restriction of late cerebral cortical progenitors to an upper-layer fate, Neuron. 17 (1996) 55–61. doi:10.1016/S0896-6273(00)80280-9.
[23] R.F. Hevner, R.A.M. Daza, J.L.R. Rubenstein, H. Stunnenberg, J.F. Olavarria, C. Englund, Beyond laminar fate: Toward a molecular classification of cortical projection/pyramidal neurons, Dev. Neurosci. 25 (2003) 139–151. doi:10.1159/000072263.
[24] T. Kumamoto, K. ichi Toma, Gunadi, W.L. McKenna, T. Kasukawa, S. Katzman, B. Chen, C. Hanashima, Foxg1 coordinates the switch from nonradially to radially migrating glutamatergic subtypes in the neocortex through spatiotemporal repression, Cell Rep. 3 (2013) 931–945. doi:10.1016/j.celrep.2013.02.023.
[25] W.L. McKenna, J. Betancourt, K.A. Larkin, B. Abrams, C. Guo, J.L. Rubenstein, B. Chen, Tbr1 and Fezf2 regulate alternate corticofugal neuronal identities during neocortical development, J Neurosci. 31 (2011) 549–564. doi:10.1523/JNEUROSCI.4131-10.2011.
[26] K. Toma, T. Kumamoto, C. Hanashima, The timing of upper-layer neurogenesis is conferred by sequential derepression and negative feedback from deep-layer neurons, J Neurosci. 34 (2014) 13259–13276. doi:10.1523/JNEUROSCI.2334-14.2014.
[27] E.A. Alcamo, L. Chirivella, M. Dautzenberg, G. Dobreva, I. Fari??as, R. Grosschedl, S.K. McConnell, Satb2 Regulates Callosal Projection Neuron Identity in the Developing Cerebral Cortex, Neuron. 57 (2008) 364–377. doi:10.1016/j.neuron.2007.12.012.
[28] Y. Sugitani, S. Nakai, O. Minowa, M. Nishi, K.I. Jishage, H. Kawano, K. Mori, M. Ogawa, T. Noda, Brn-1 and Brn-2 share crucial roles in the production and positioning of mouse neocortical neurons, Genes Dev. 16 (2002) 1760–1765. doi:10.1101/gad.978002.
[29] M. Nieto, C. Schuurmans, O. Britz, F. Guillemot, Neural bHLH genes control the neuronal versus glial fate decision in cortical progenitors, Neuron. 29 (2001) 401–413. doi:10.1016/S0896-6273(01)00214-8.
[30] A. Bonni, Y. Sun, M. Nadal-Vicens, A. Bhatt, D.A. Frank, I. Rozovsky, N. Stahl, G.D. Yancopoulos, M.E. Greenberg, Regulation of Gliogenesis in the Central Nervous System by the JAK-STAT Signaling Pathway, Science (80-.). 278 (1997) 477–483. doi:10.1126/science.278.5337.477.
[31] F. Barnabé-Heider, J.A. Wasylnka, K.J.L. Fernandes, C. Porsche, M. Sendtner, D.R. Kaplan, F.D. Miller, Evidence that embryonic neurons regulate the onset of cortical gliogenesis via cardiotrophin-1, Neuron. 48 (2005) 253–265. doi:10.1016/j.neuron.2005.08.037.
[32] S.A. Koblar, A.M. Turnley, B.J. Classon, K.L. Reid, C.B. Ware, S.S. Cheema, M. Murphy, P.F. Bartlett, Neural precursor differentiation into astrocytes requires signaling through the leukemia inhibitory factor receptor., Proc. Natl. Acad. Sci. U.

S. A. 95 (1998) 3178–81. doi:10.1073/pnas.95.6.3178.
[33] K. Nakashima, S. Wiese, M. Yanagisawa, H. Arakawa, N. Kimura, T. Hisatsune, K. Yoshida, T. Kishimoto, M. Sendtner, T. Taga, Developmental requirement of gp130 signaling in neuronal survival and astrocyte differentiation., J. Neurosci. 19 (1999) 5429–5434.
[34] Alton Eduard d', Döllinger Ignaz, Pander Christian Heinrich, Beiträge zur Entwickelungsgeschichte des Hühnchens im Eye /, 2015. doi:10.5962/bhl.title.106814.
[35] H. Spemann, Über die Determination der ersten Organanlagen des Amphibienembryo I-VI, Arch. Für Entwicklungsmechanik Der Org. (1918). doi:10.1007/BF02267308.
[36] H. Spemann, H. Mangold, über Induktion von Embryonalanlagen durch Implantation artfremder Organisatoren, Arch. Für Mikroskopische Anat. Und Entwicklungsmechanik. (1924). doi:10.1007/BF02108133.
[37] K.A. Moore, I.R. Lemischka, Stem cells and their niches., Science. 311 (2006) 1880–5. doi:10.1126/science.1110542.
[38] A.J. Engler, S. Sen, H.L. Sweeney, D.E. Discher, Matrix elasticity directs stem cell lineage specification., Cell. 126 (2006) 677–89. doi:10.1016/j.cell.2006.06.044.
[39] R. Schofield, The relationship between the spleen colony-forming cell and the haemopoietic stem cell., Blood Cells. 4 (1978) 7–25.
[40] J. Barthes, H. Özçelik, M. Hindié, A. Ndreu-Halili, A. Hasan, N.E. Vrana, Cell Microenvironment Engineering and Monitoring for Tissue Engineering and Regenerative Medicine: The Recent Advances, Biomed Res. Int. 2014 (2014) 921905. doi:10.1155/2014/921905.
[41] P.C. Sachs, P.A. Mollica, R.D. Bruno, Tissue specific microenvironments: A key tool for tissue engineering and regenerative medicine, J. Biol. Eng. 11 (2017) 34. doi:10.1186/s13036-017-0077-0.
[42] D. Hanahan, R. a Weinberg, Hallmarks of cancer: the next generation., Cell. 144 (2011) 646–74. doi:10.1016/j.cell.2011.02.013.
[43] C. Streuli, Extracellular matrix remodelling and cellular differentiation, Curr. Opin. Cell Biol. 11 (1999) 634–640. doi:10.1016/S0955-0674(99)00026-5.
[44] A.I. Teixeira, S. Ilkhanizadeh, J.A. Wigenius, J.K. Duckworth, O. Inganäs, O. Hermanson, The promotion of neuronal maturation on soft substrates, Biomaterials. 30 (2009) 4567–4572. doi:10.1016/j.biomaterials.2009.05.013.
[45] E. Garcion, A. Halilagic, A. Faissner, C. ffrench-Constant, Generation of an environmental niche for neural stem cell development by the extracellular matrix molecule tenascin C., Development. 131 (2004) 3423–3432. doi:10.1242/dev.01202.
[46] M.J. Bissell, H.G. Hall, G. Parry, How does the extracellular matrix direct gene expression?, J. Theor. Biol. (1982). doi:10.1016/0022-5193(82)90388-5.
[47] V. Vogel, M. Sheetz, Local force and geometry sensing regulate cell functions, Nat. Rev. Mol. Cell Biol. 7 (2006) 265–275. doi:10.1038/nrm1890.
[48] J.M. Barnes, L. Przybyla, V.M. Weaver, Tissue mechanics regulate brain development, homeostasis and disease, J. Cell Sci. 130 (2017) 71–82. doi:10.1242/jcs.191742.
[49] M. Iwashita, N. Kataoka, K. Toida, Y. Kosodo, Systematic profiling of spatiotemporal tissue and cellular stiffness in the developing brain, Dev. 141 (2014) 3793–3798. doi:10.1242/dev.109637.
[50] K. Saha, A.J. Keung, E.F. Irwin, Y. Li, L. Little, D. V Schaffer, K.E. Healy, Substrate modulus directs neural stem cell behavior., Biophys. J. 95 (2008) 4426–38. doi:10.1529/biophysj.108.132217.
[51] K.A. Kilian, B. Bugarija, B.T. Lahn, M. Mrksich, Geometric cues for directing the differentiation of mesenchymal stem cells., Proc. Natl. Acad. Sci. U. S. A. 107

(2010) 4872–7. doi:10.1073/pnas.0903269107.
[52] M. Poudineh, Z. Wang, M. Labib, M. Ahmadi, L. Zhang, J. Das, S. Ahmed, S. Angers, S.O. Kelley, Three-Dimensional Nanostructured Architectures Enable Efficient Neural Differentiation of Mesenchymal Stem Cells via Mechanotransduction, Nano Lett. 18 (2018) 7188–7193. doi:10.1021/acs.nanolett.8b03313.
[53] N.R. Blumenthal, O. Hermanson, B. Heimrich, V.P. Shastri, Stochastic nanoroughness modulates neuron–astrocyte interactions and function via mechanosensing cation channels, Proc. Natl. Acad. Sci. 111 (2014) 16124–16129. doi:10.1073/pnas.1412740111.
[54] R. Edmondson, J.J. Broglie, A.F. Adcock, L. Yang, Three-dimensional cell culture systems and their applications in drug discovery and cell-based biosensors., Assay Drug Dev. Technol. 12 (2014) 207–18. doi:10.1089/adt.2014.573.
[55] F. Grinnell, C.-H. Ho, E. Tamariz, D.J. Lee, G. Skuta, Dendritic fibroblasts in three-dimensional collagen matrices., Mol. Biol. Cell. 14 (2003) 384–95. doi:10.1091/mbc.e02-08-0493.
[56] E. Cukierman, R. Pankov, D.R. Stevens, K.M. Yamada, Taking cell-matrix adhesions to the third dimension, Science (80-.). (2001). doi:10.1126/science.1064829.
[57] A. Domogatskaya, S. Rodin, K. Tryggvason, Functional Diversity of Laminins, Annu. Rev. Cell Dev. Biol. 28 (2012) 523–553. doi:10.1146/annurev-cellbio-101011-155750.
[58] E. Hohenester, P.D. Yurchenco, Laminins in basement membrane assembly, Cell Adhes. Migr. 7 (2013) 56–63. doi:10.4161/cam.21831.
[59] P.E. Hall, J.D. Lathia, M.A. Caldwell, C. Ffrench-Constant, Laminin enhances the growth of human neural stem cells in defined culture media., BMC Neurosci. 9 (2008) 71. doi:10.1186/1471-2202-9-71.
[60] L.A. Flanagan, L.M. Rebaza, S. Derzic, P.H. Schwartz, E.S. Monuki, Regulation of Human Neural Precursor Cells by Laminin and Integrins, J. Neurosci. Res. 83 (2006) 845. doi:10.1002/JNR.20778.
[61] W. Ma, T. Tavakoli, E. Derby, Y. Serebryakova, M.S. Rao, M.P. Mattson, Cell-extracellular matrix interactions regulate neural differentiation of human embryonic stem cells., BMC Dev. Biol. 8 (2008) 90. doi:10.1186/1471-213X-8-90.
[62] S.L. Bellis, Advantages of RGD peptides for directing cell association with biomaterials, Biomaterials. 32 (2011) 4205–4210. doi:10.1016/j.biomaterials.2011.02.029.
[63] M.C. Simon, B. Keith, The role of oxygen availability in embryonic development and stem cell function., Nat. Rev. Mol. Cell Biol. 9 (2008) 285–96. doi:10.1038/nrm2354.
[64] F. Rodesch, P. Simon, C. Donner, E. Jauniaux, Oxygen measurements in endometrial and trophoblastic tissues during early pregnancy., Obstet. Gynecol. 80 (1992) 283–285.
[65] T. Ezashi, P. Das, R.M. Roberts, Low O2 tensions and the prevention of differentiation of hES cells., Proc. Natl. Acad. Sci. U. S. A. 102 (2005) 4783–8. doi:10.1073/pnas.0501283102.
[66] G.L. Wang, B.H. Jiang, E.A. Rue, G.L. Semenza, Hypoxia-inducible factor 1 is a basic-helix-loop-helix-PAS heterodimer regulated by cellular O2 tension, Proc. Natl. Acad. Sci. U. S. A. 92 (1995) 5510–5514. doi:10.1073/pnas.92.12.5510.
[67] L.E. Huang, J. Gu, M. Schau, H.F. Bunn, Regulation of hypoxia-inducible factor 1alpha is mediated by an O2-dependent degradation domain via the ubiquitin-proteasome pathway., Proc. Natl. Acad. Sci. U. S. A. 95 (1998) 7987–92. doi:10.1073/pnas.95.14.7987.

[68] F.R. Sharp, M. Bernaudin, HIF1 and oxygen sensing in the brain, Nat. Rev. Neurosci. 5 (2004) 437–448. doi:10.1038/nrn1408.
[69] M. V. Gustafsson, X. Zheng, T. Pereira, K. Gradin, S. Jin, J. Lundkvist, J.L. Ruas, L. Poellinger, U. Lendahl, M. Bondesson, S. Artavanis-Tsakonas, M.D. Rand, R.J. Lake, W. Balkan, M.A. Tavianini, P.J. Gkonos, A.J. Giaccia, et al., Hypoxia Requires Notch Signaling to Maintain the Undifferentiated Cell State, Dev. Cell. 9 (2005) 617–628. doi:10.1016/j.devcel.2005.09.010.
[70] T. Mutoh, T. Sanosaka, K. Ito, K. Nakashima, Oxygen Levels Epigenetically Regulate Fate Switching of Neural Precursor Cells via Hypoxia-Inducible Factor 1α-Notch Signal Interaction in the Developing Brain, Stem Cells. 30 (2012) 561–569. doi:10.1002/stem.1019.
[71] L. Figueiredo, R. Pace, C. D'Arros, G. Réthoré, J. Guicheux, C. Le Visage, P. Weiss, Assessing glucose and oxygen diffusion in hydrogels for the rational design of 3D stem cell scaffolds in regenerative medicine, J. Tissue Eng. Regen. Med. 12 (2018) 1238–1246. doi:10.1002/term.2656.
[72] A.G. Ardakani, U. Cheema, R.A. Brown, R.J. Shipley, Quantifying the correlation between spatially defined oxygen gradients and cell fate in an engineered three-dimensional culture model, J. R. Soc. Interface. 11 (2014) 20140501. doi:10.1098/rsif.2014.0501.
[73] V. Kumar, J.E. Carlson, K.A. Ohgi, T.A. Edwards, D.W. Rose, C.R. Escalante, M.G. Rosenfeld, A.K. Aggarwal, Transcription corepressor CtBP is an NAD+-regulated dehydrogenase, Mol. Cell. 10 (2002) 857–869. doi:10.1016/S1097-2765(02)00650-0.
[74] C. Bhambhani, J.L. Chang, D.L. Akey, K.M. Cadigan, The oligomeric state of CtBP determines its role as a transcriptional co-activator and co-repressor of Wingless targets, EMBO J. 30 (2011) 2031–2043. doi:10.1038/emboj.2011.100.
[75] P. Balasubramanian, L.-J. Zhao, G. Chinnadurai, Nicotinamide adenine dinucleotide stimulates oligomerization, interaction with adenovirus E1A and an intrinsic dehydrogenase activity of CtBP, FEBS Lett. 537 (2003) 157–160. doi:10.1016/S0014-5793(03)00119-4.
[76] Q. Zhang, D.W. Piston, R.H. Goodman, Regulation of corepressor function by nuclear NADH., Science. 295 (2002) 1895–7. doi:10.1126/science.1069300.
[77] A.G. Bellesis, A.M. Jecrois, J.A. Hayes, C.A. Schiffer, W.E. Royer, Assembly of human C-terminal binding protein (CtBP) into tetramers, J. Biol. Chem. 293 (2018) 9101–9112. doi:10.1074/jbc.RA118.002514.
[78] J.D. Hildebrand, P. Soriano, Overlapping and Unique Roles for C-Terminal Binding Protein 1 (CtBP1) and CtBP2 during Mouse Development., Mol. Cell. Biol. 22 (2002) 5296–5307. doi:10.1128/mcb.22.15.5296-5307.2002.
[79] G. Chinnadurai, The Transcriptional Corepressor CtBP: A Foe of Multiple Tumor Suppressors, Cancer Res. 69 (2009) 731–734. doi:10.1158/0008-5472.can-08-3349.
[80] S.S. Levine, I.F.G. King, R.E. Kingston, Division of labor in Polycomb group repression, Trends Biochem. Sci. (2004). doi:10.1016/j.tibs.2004.07.007.
[81] J.H. Kim, E.J. Cho, S.T. Kim, H.D. Youn, CtBP represses p300-mediated transcriptional activation by direct association with its bromodomain, Nat. Struct. Mol. Biol. (2005). doi:10.1038/nsmb924.
[82] Q. Zhang, S.-Y. Wang, A.C. Nottke, J. V. Rocheleau, D.W. Piston, R.H. Goodman, Redox sensor CtBP mediates hypoxia-induced tumor cell migration, Proc. Natl. Acad. Sci. (2006). doi:10.1073/pnas.0603269103.
[83] L. Barroilhet, J. Yang, K. Hasselblatt, R.M. Paranal, S.K. Ng, J.A. Rauh-Hain, W.R. Welch, J.E. Bradner, R.S. Berkowitz, S.W. Ng, C-terminal binding protein-2 regulates response of epithelial ovarian cancer cells to histone deacetylase inhibitors, Oncogene. (2013). doi:10.1038/onc.2012.380.

[84] L.-J. Di, J.S. Byun, M.M. Wong, C. Wakano, T. Taylor, S. Bilke, S. Baek, K. Hunter, H. Yang, M. Lee, C. Zvosec, G. Khramtsova, F. Cheng, C.M. Perou, C. Ryan Miller, R. Raab, O.I. Olopade, K. Gardner, Genome-wide profiles of CtBP link metabolism with genome stability and epithelial reprogramming in breast cancer, Nat. Commun. 4 (2013) 1449. doi:10.1038/ncomms2438.
[85] J.M. Dias, S. Ilkhanizadeh, E. Karaca, J.K. Duckworth, V. Lundin, M.G. Rosenfeld, J. Ericson, O. Hermanson, A.I. Teixeira, CtBPs sense microenvironmental oxygen levels to regulate neural stem cell state, Cell Rep. 8 (2014) 665–670. doi:10.1016/j.celrep.2014.06.057.
[86] J. Koipally, K. Georgopoulos, Ikaros interactions with CtBP reveal a repression mechanism that is independent of histone deacetylase activity, J. Biol. Chem. (2000). doi:10.1074/jbc.M000254200.
[87] J.M. Alsio, B. Tarchini, M. Cayouette, F.J. Livesey, Ikaros promotes early-born neuronal fates in the cerebral cortex, Proc. Natl. Acad. Sci. 110 (2013) E716–E725. doi:10.1073/pnas.1215707110.
[88] H. Wang, Z. Xiao, J. Zheng, J. Wu, X.L. Hu, X. Yang, Q. Shen, ZEB1 Represses Neural Differentiation and Cooperates with CTBP2 to Dynamically Regulate Cell Migration during Neocortex Development, Cell Rep. 27 (2019) 2335-2353.e6. doi:10.1016/j.celrep.2019.04.081.
[89] D.R. Powell, A.J. Blasky, S.G. Britt, K.B. Artinger, Riding the crest of the wave: Parallels between the neural crest and cancer in epithelial-to-mesenchymal transition and migration, Wiley Interdiscip. Rev. Syst. Biol. Med. (2013). doi:10.1002/wsbm.1224.
[90] A.M. Handorf, Y. Zhou, M.A. Halanski, W.J. Li, Tissue stiffness dictates development, homeostasis, and disease progression, Organogenesis. 11 (2015) 1–15. doi:10.1080/15476278.2015.1019687.
[91] J.I. Johnsen, C. Dyberg, M. Wickström, Neuroblastoma—A Neural Crest Derived Embryonal Malignancy, Front. Mol. Neurosci. 12 (2019) 9. doi:10.3389/fnmol.2019.00009.
[92] I. Tadeo, A.P. Berbegall, V. Castel, P. García-Miguel, R. Callaghan, S. Påhlman, S. Navarro, R. Noguera, Extracellular matrix composition defines an ultra-high-risk group of neuroblastoma within the high-risk patient cohort., Br. J. Cancer. 115 (2016) 480–9. doi:10.1038/bjc.2016.210.
[93] W.A. Lam, L. Cao, V. Umesh, A.J. Keung, S. Sen, S. Kumar, Extracellular matrix rigidity modulates neuroblastoma cell differentiation and N-myc expression, Mol. Cancer. 9 (2010) 35. doi:10.1186/1476-4598-9-35.
[94] G.N. Li, L.L. Livi, C.M. Gourd, E.S. Deweerd, D. Hoffman-Kim, Genomic and morphological changes of neuroblastoma cells in response to three-dimensional matrices., Tissue Eng. 13 (2007) 1035–1047. doi:10.1089/ten.2006.0251.
[95] L. Loeb, Uber die Entstehung von Bindegewebe, Leukocyten und roten Blutkorperchen aus Epithel und uber eine Methode, isolierte Gewebsteile zu zuchten, Stern. (1897).
[96] M. Amit, M.K. Carpenter, M.S. Inokuma, C.P. Chiu, C.P. Harris, M. a Waknitz, J. Itskovitz-Eldor, J. a Thomson, Clonally derived human embryonic stem cell lines maintain pluripotency and proliferative potential for prolonged periods of culture., Dev. Biol. 227 (2000) 271–278. doi:10.1006/dbio.2000.9912.
[97] F.G. Heineken, R. Skalak, Tissue Engineering: A Brief Overview, J. Biomech. Eng. 113 (1991) 111. doi:10.1115/1.2891223.
[98] R. Langer, J. Vacanti, Tissue engineering, Science (80-.). 260 (1993) 920–926. doi:10.1126/science.8493529.
[99] Y. Peck, D.-A. Wang, Three-dimensionally engineered biomimetic tissue models for in vitro drug evaluation: delivery, efficacy and toxicity., Expert Opin. Drug Deliv. 10

(2013) 369–83. doi:10.1517/17425247.2013.751096.
[100] J.E. Nichols, J.A. Niles, S.P. Vega, L.B. Argueta, A. Eastaway, J. Cortiella, Modeling the lung: Design and development of tissue engineered macro- and micro-physiologic lung models for research use., Exp. Biol. Med. (Maywood). 239 (2014) 1135–69. doi:10.1177/1535370214536679.
[101] J.S. Theodoropoulos, J.N.A. De Croos, S.S. Park, R. Pilliar, R.A. Kandel, Integration of tissue-engineered cartilage with host cartilage: an in vitro model., Clin. Orthop. Relat. Res. 469 (2011) 2785–95. doi:10.1007/s11999-011-1856-4.
[102] C.E. Murry, G. Keller, Differentiation of embryonic stem cells to clinically relevant populations: lessons from embryonic development., Cell. 132 (2008) 661–80. doi:10.1016/j.cell.2008.02.008.
[103] R. McBeath, D.M. Pirone, C.M. Nelson, K. Bhadriraju, C.S. Chen, Cell Shape, Cytoskeletal Tension, and RhoA Regulate Stem Cell Lineage Commitment, Dev. Cell. 6 (2004) 483–495. doi:10.1016/S1534-5807(04)00075-9.
[104] W.-J.W.-J. Li, R. Tuli, C. Okafor, A. Derfoul, K.G.K.G. Danielson, D.J.D.J. Hall, R.S.R.S. Tuan, A three-dimensional nanofibrous scaffold for cartilage tissue engineering using human mesenchymal stem cells., Biomaterials. 26 (2005) 599–609. doi:10.1016/j.biomaterials.2004.03.005.
[105] A. Atala, S.B. Bauer, S. Soker, J.J. Yoo, A.B. Retik, Tissue-engineered autologous bladders for patients needing cystoplasty, Lancet. 367 (2006) 1241–1246.
[106] P. Macchiarini, P. Jungebluth, T. Go, M. Asnaghi, L.E. Rees, T.A. Cogan, A. Dodson, J. Martorell, S. Bellini, P.P. Parnigotto, Clinical transplantation of a tissue-engineered airway, Lancet. 372 (2008) 2023–2030.
[107] E. Sachlos, J.T. Czernuszka, Making tissue engineering scaffolds work. Review: the application of solid freeform fabrication technology to the production of tissue engineering scaffolds., Eur. Cell. Mater. 5 (2003) 29–40.
[108] B. Derby, Printing and prototyping of tissues and scaffolds., Science. 338 (2012) 921–926. doi:10.1126/science.1226340.
[109] H.Y. Chang, Anatomic demarcation of cells: genes to patterns., Science. 326 (2009) 1206–7. doi:10.1126/science.1175686.
[110] Y. Xia, G.M. Whitesides, Soft Lithography, Angew. Chemie Int. Ed. 37 (1998) 550–575. doi:10.1002/(SICI)1521-3773(19980316)37:5<550::AID-ANIE550>3.0.CO;2-G.
[111] H. Clevers, Modeling Development and Disease with Organoids., Cell. 165 (2016) 1586–1597. doi:10.1016/j.cell.2016.05.082.
[112] W. Peng, P. Datta, Y. Wu, M. Dey, B. Ayan, A. Dababneh, I.T. Ozbolat, Challenges in bio-fabrication of organoid cultures, in: Adv. Exp. Med. Biol., Springer, Cham, 2018: pp. 53–71. doi:10.1007/5584_2018_216.
[113] B. Derby, V. Mironov, D.N. Reis, Review: Bioprinting A Beginning, (2006).
[114] R.J. Klebe, Cytoscribing: a method for micropositioning cells and the construction of two- and three-dimensional synthetic tissues., Exp. Cell Res. 179 (1988) 362–373. doi:10.1016/0014-4827(88)90275-3.
[115] W.C. Wilson, T. Boland, Cell and organ printing 1: protein and cell printers., Anat. Rec. A. Discov. Mol. Cell. Evol. Biol. 272 (2003) 491–496. doi:10.1002/ar.a.10057.
[116] C.W. Hull, Apparatus for Production of Three-Dimensional Objects by Stereolithography, in: Google Patents, 1986.
[117] C.M. Smith, A.L. Stone, R.L. Parkhill, R.L. Stewart, M.W. Simpkins, A.M. Kachurin, W.L. Warren, S.K. Williams, Three-dimensional bioassembly tool for generating viable tissue-engineered constructs., Tissue Eng. 10 (2004) 1566–76. doi:10.1089/ten.2004.10.1566.
[118] Y.-B. Lee, S. Polio, W. Lee, G. Dai, L. Menon, R.S. Carroll, S.-S. Yoo, Bio-printing of collagen and VEGF-releasing fibrin gel scaffolds for neural stem cell culture, Exp.

Neurol. 223 (2010) 645–652. doi:10.1016/j.expneurol.2010.02.014.
[119] R. Chang, J. Nam, W. Sun, Effects of dispensing pressure and nozzle diameter on cell survival from solid freeform fabrication-based direct cell writing., Tissue Eng. Part A. 14 (2008) 41–8. doi:10.1089/ten.a.2007.0004.
[120] K. Jakab, B. Damon, A. Neagu, A. Kachurin, G. Forgacs, Three-dimensional tissue constructs built by bioprinting, Biorheology. 43 (2006) 509–513.
[121] S. V Murphy, A. Atala, 3D bioprinting of tissues and organs., Nat. Biotechnol. 32 (2014) 773–785. doi:10.1038/nbt.2958.
[122] S.M. Peltola, F.P.W. Melchels, D.W. Grijpma, M. Kellomäki, A review of rapid prototyping techniques for tissue engineering purposes., Ann. Med. 40 (2008) 268–80. doi:10.1080/07853890701881788.
[123] C.J. Ferris, K.G. Gilmore, G.G. Wallace, M. In het Panhuis, Biofabrication: an overview of the approaches used for printing of living cells., Appl. Microbiol. Biotechnol. 97 (2013) 4243–58. doi:10.1007/s00253-013-4853-6.
[124] W. Schuurman, P.A. Levett, M.W. Pot, P.R. van Weeren, W.J.A. Dhert, D.W. Hutmacher, F.P.W. Melchels, T.J. Klein, J. Malda, Gelatin-methacrylamide hydrogels as potential biomaterials for fabrication of tissue-engineered cartilage constructs., Macromol. Biosci. 13 (2013) 551–61. doi:10.1002/mabi.201200471.
[125] M. Xu, X. Wang, Y. Yan, R. Yao, Y. Ge, An cell-assembly derived physiological 3D model of the metabolic syndrome, based on adipose-derived stromal cells and a gelatin/alginate/fibrinogen matrix., Biomaterials. 31 (2010) 3868–77. doi:10.1016/j.biomaterials.2010.01.111.
[126] S. Moon, S.K. Hasan, Y.S. Song, F. Xu, H.O. Keles, F. Manzur, S. Mikkilineni, J.W. Hong, J. Nagatomi, E. Haeggstrom, A. Khademhosseini, U. Demirci, Layer by layer three-dimensional tissue epitaxy by cell-laden hydrogel droplets., Tissue Eng. Part C. Methods. 16 (2010) 157–166. doi:10.1089/ten.tec.2009.0179.
[127] J. Malda, J. Visser, F.P. Melchels, T. Jüngst, W.E. Hennink, W.J. a Dhert, J. Groll, D.W. Hutmacher, 25th anniversary article: Engineering hydrogels for biofabrication, Adv. Mater. 25 (2013) 5011–5028. doi:10.1002/adma.201302042.
[128] Y.B. Lee, S. Polio, W. Lee, G. Dai, L. Menon, R.S. Carroll, S.S. Yoo, Bio-printing of collagen and VEGF-releasing fibrin gel scaffolds for neural stem cell culture, Exp. Neurol. 223 (2010) 645–652. doi:10.1016/j.expneurol.2010.02.014.
[129] V.K. Lee, A.M. Lanzi, H. Ngo, S.-S. Yoo, P.A. Vincent, G. Dai, Generation of Multi-scale Vascular Network System Within 3D Hydrogel Using 3D Bio-printing Technology, Cel. Mol. Bioeng. 7 (2014) 460–472. doi:10.1007/s12195-014-0340-0.
[130] C. Hydrogel, D. Assembling, Y.O.Y. An, H.A.L. Iu, R.E.Z. Hang, Direct Fabrication of a Hybrid Cell/Hydrogel Construct by a Double-nozzle Assembling Technology, J. Bioact. Compat. Polym. 24 (2009) 249–265. doi:10.1177/0883911509104094.
[131] S.J. Kalita, S. Bose, H.L. Hosick, A. Bandyopadhyay, Development of controlled porosity polymer-ceramic composite scaffolds via fused deposition modeling, Mater. Sci. Eng. C. 23 (2003) 611–620. doi:10.1016/S0928-4931(03)00052-3.
[132] V. Mironov, R.P. Visconti, V. Kasyanov, G. Forgacs, C.J. Drake, R.R. Markwald, Organ printing: tissue spheroids as building blocks., Biomaterials. 30 (2009) 2164–74. doi:10.1016/j.biomaterials.2008.12.084.
[133] Y. Luo, X. Wei, P. Huang, 3D bioprinting of hydrogel-based biomimetic microenvironments, J. Biomed. Mater. Res. - Part B Appl. Biomater. 107 (2019) 1695–1705. doi:10.1002/jbm.b.34262.
[134] W. Lee, J.C. Debasitis, V.K. Lee, J.-H. Lee, K. Fischer, K. Edminster, J.-K. Park, S.-S. Yoo, Multi-layered culture of human skin fibroblasts and keratinocytes through three-dimensional freeform fabrication., Biomaterials. 30 (2009) 1587–95. doi:10.1016/j.biomaterials.2008.12.009.
[135] A.E. Jakus, A.L. Rutz, S.W. Jordan, A. Kannan, S.M. Mitchell, C. Yun, K.D. Koube,

S.C. Yoo, H.E. Whiteley, C.-P. Richter, R.D. Galiano, W.K. Hsu, S.R. Stock, E.L. Hsu, R.N. Shah, Hyperelastic "bone": A highly versatile, growth factor-free, osteoregenerative, scalable, and surgically friendly biomaterial., Sci. Transl. Med. 8 (2016) 358ra127. doi:10.1126/scitranslmed.aaf7704.

[136] L. Gao, M.E. Kupfer, J.P. Jung, L. Yang, P. Zhang, Y. Da Sie, Q. Tran, V. Ajeti, B.T. Freeman, V.G. Fast, P.J. Campagnola, B.M. Ogle, J. Zhang, Myocardial Tissue Engineering with Cells Derived from Human-Induced Pluripotent Stem Cells and a Native-Like, High-Resolution, 3-Dimensionally Printed Scaffold, Circ. Res. 120 (2017) 1318–1325. doi:10.1161/CIRCRESAHA.116.310277.

[137] K. Kang, Y. Kim, H. Jeon, S.B. Lee, J.S. Kim, S.A. Park, W.D. Kim, H.M. Yang, S.J. Kim, J. Jeong, D. Choi, Three-Dimensional Bioprinting of Hepatic Structures with Directly Converted Hepatocyte-Like Cells, Tissue Eng. Part A. 24 (2017) 576–583. doi:10.1089/ten.tea.2017.0161.

[138] J. Arrowsmith, P. Miller, Trial Watch: Phase II and Phase III attrition rates 2011-2012, Nat. Rev. Drug Discov. (2013). doi:10.1038/nrd4090.

[139] D. Loessner, K.S. Stok, M.P. Lutolf, D.W. Hutmacher, J.A. Clements, S.C. Rizzi, Bioengineered 3D platform to explore cell-ECM interactions and drug resistance of epithelial ovarian cancer cells, Biomaterials. 31 (2010) 8494–8506. doi:10.1016/j.biomaterials.2010.07.064.

[140] M.A. Heinrich, R. Bansal, T. Lammers, Y.S. Zhang, R. Michel Schiffelers, J. Prakash, 3D-Bioprinted Mini-Brain: A Glioblastoma Model to Study Cellular Interactions and Therapeutics, Adv. Mater. 31 (2019). doi:10.1002/adma.201806590.

[141] M. Duchamp, T. Liu, A.M. Genderen, V. Kappings, R. Oklu, L.W. Ellisen, Y.S. Zhang, Sacrificial Bioprinting of a Mammary Ductal Carcinoma Model, Biotechnol. J. (2019) 1700703. doi:10.1002/biot.201700703.

[142] F. Meng, C.M. Meyer, D. Joung, D.A. Vallera, M.C. McAlpine, A. Panoskaltsis-Mortari, 3D Bioprinted In Vitro Metastatic Models via Reconstruction of Tumor Microenvironments, Adv. Mater. 31 (2019) 1806899. doi:10.1002/adma.201806899.

[143] K.L. Spiller, S.A. Maher, A.M. Lowman, Hydrogels for the Repair of Articular Cartilage Defects, Http://Www.Liebertpub.Com/Teb. (2011). doi:10.1089/TEN.TEB.2011.0077.

[144] N.C. Hunt, L.M. Grover, Cell encapsulation using biopolymer gels for regenerative medicine, Biotechnol. Lett. 32 (2010) 733–742. doi:10.1007/s10529-010-0221-0.

[145] M. Dash, F. Chiellini, R.M. Ottenbrite, E. Chiellini, Chitosan—A versatile semi-synthetic polymer in biomedical applications, Prog. Polym. Sci. 36 (2011) 981–1014. doi:10.1016/j.progpolymsci.2011.02.001.

[146] D. Seliktar, P.C. Nicolson, J. Vogt, T.B. Reece, T.S. Maxey, I.L. Kron, K.Y. Lee, D.J. Mooney, G. Kogan, L. Soltés, R. Stern, P. Gemeiner, M.W. Tibbitt, K.S. Anseth, M.P. Lutolf, P.M. Gilbert, N. Huebsch, et al., Designing cell-compatible hydrogels for biomedical applications., Science. 336 (2012) 1124–8. doi:10.1126/science.1214804.

[147] N.E. Fedorovich, J.R. De Wijn, A.J. Verbout, J. Alblas, W.J.A. Dhert, Three-dimensional fiber deposition of cell-laden, viable, patterned constructs for bone tissue printing., Tissue Eng. Part A. 14 (2008) 127–33. doi:10.1089/ten.a.2007.0158.

[148] C.A. DeForest, K.S. Anseth, Advances in bioactive hydrogels to probe and direct cell fate., Annu. Rev. Chem. Biomol. Eng. 3 (2012) 421–44. doi:10.1146/annurev-chembioeng-062011-080945.

[149] K.Y. Lee, D.J. Mooney, Alginate: Properties and biomedical applications, Prog. Polym. Sci. 37 (2012) 106–126. doi:10.1016/j.progpolymsci.2011.06.003.

[150] G.T. Grant, E.R. Morris, D.A. Rees, P.J.C. Smith, D. Thom, Biological interactions between polysaccharides and divalent cations: The egg-box model, FEBS Lett. (1973). doi:10.1016/0014-5793(73)80770-7.

[151] F. Lim, A.M. Sun, Microencapsulated islets as bioartificial endocrine pancreas, Science (80-.). 210 (1980) 908–910. doi:10.1126/science.6776628.
[152] X. Huang, X. Zhang, X. Wang, C. Wang, B. Tang, Microenvironment of alginate-based microcapsules for cell culture and tissue engineering, J. Biosci. Bioeng. 114 (2012) 1–8. doi:10.1016/j.jbiosc.2012.02.024.
[153] K.Y. Lee, D.J. Mooney, J.A. Rowley, G. Madlambayan, D.J. Mooney, Alginate hydrogels as synthetic extracellular matrix materials, Biomaterials. 20 (2011) 45–53. doi:10.1016/j.progpolymsci.2011.06.003.
[154] C. Tamponnet, S. Boisseau, P.-N. Lirsac, J.-N. Barbotin, C. Poujeol, M. Lievremont, M. Simonneau, Storage and growth of neuroblastoma cells immobilized in calcium-alginate beads, Appl. Microbiol. Biotechnol. 33 (1990) 442–447. doi:10.1007/BF00176662.
[155] Q. Gao, Y. He, J. zhong Fu, A. Liu, L. Ma, Coaxial nozzle-assisted 3D bioprinting with built-in microchannels for nutrients delivery, Biomaterials. 61 (2015) 203–215. doi:10.1016/j.biomaterials.2015.05.031.
[156] T.J. Hinton, Q. Jallerat, R.N. Palchesko, J.H. Park, M.S. Grodzicki, H.-J. Shue, M.H. Ramadan, A.R. Hudson, A.W. Feinberg, Three-dimensional printing of complex biological structures by freeform reversible embedding of suspended hydrogels, Sci. Adv. 1 (2015) e1500758–e1500758. doi:10.1126/sciadv.1500758.
[157] I.I. Agapov, O.L. Pustovalova, M.M. Moisenovich, V.G. Bogush, O.S. Sokolova, V.I. Sevastyanov, V.G. Debabov, M.P. Kirpichnikov, Three-dimensional scaffold made from recombinant spider Silk protein for tissue engineering, 426 (2009) 127–130. doi:10.1134/S1607672909030016.
[158] M.Y. Hedhammar, H. Bramfeldt, T. Baris, M. Widhe, G. Askarieh, K. Nordling, S. Von Aulock, J. Johansson, Sterilized recombinant spider silk fibers of low pyrogenicity, Biomacromolecules. 11 (2010) 953–959. doi:10.1021/bm9014039.
[159] E. Bini, C.W.P. Foo, J. Huang, V. Karageorgiou, B. Kitchel, D.L. Kaplan, RGD-functionalized bioengineered spider dragline silk biomaterial, Biomacromolecules. 7 (2006) 3139–3145. doi:10.1021/bm0607877.
[160] J. Scheller, D. Henggeler, A. Viviani, U. Conrad, Purification of spider silk-elastin from transgenic plants and application for human chondrocyte proliferation, Transgenic Res. 13 (2004) 51–57. doi:10.1023/B:TRAG.0000017175.78809.7a.
[161] L. Yang, M. Hedhammar, T. Blom, K. Leifer, J. Johansson, P. Habibovic, C. a van Blitterswijk, Biomimetic calcium phosphate coatings on recombinant spider silk fibres., Biomed. Mater. 5 (2010) 045002. doi:10.1088/1748-6041/5/4/045002.
[162] M. Lewicka, O. Hermanson, A.U. Rising, Recombinant spider silk matrices for neural stem cell cultures, Biomaterials. 33 (2012) 7712–7717. doi:10.1016/j.biomaterials.2012.07.021.
[163] C. Fredriksson, M. Hedhammar, R. Feinstein, K. Nordling, G. Kratz, J. Johansson, F. Huss, A. Rising, Tissue response to subcutaneously implanted recombinant spider silk: An in vivo study, Materials (Basel). 2 (2009) 1908–1922. doi:10.3390/ma2041908.
[164] L. Baoyong, Z. Jian, C. Denglong, L. Min, Evaluation of a new type of wound dressing made from recombinant spider silk protein using rat models., Burns. 36 (2010) 891–6. doi:10.1016/j.burns.2009.12.001.
[165] M. Widhe, H. Bysell, S. Nystedt, I. Schenning, M. Malmsten, J. Johansson, A. Rising, M. Hedhammar, Recombinant spider silk as matrices for cell culture., Biomaterials. 31 (2010) 9575–9585. doi:10.1016/j.biomaterials.2010.08.061.
[166] K. Schacht, T. Jüngst, M. Schweinlin, A. Ewald, J. Groll, T. Scheibel, Biofabrication of Cell-Loaded 3D Spider Silk Constructs, Angew. Chemie Int. Ed. 54 (2015) 2816–2820. doi:10.1002/anie.201409846.
[167] A. Rising, J. Johansson, Toward spinning artificial spider silk, Nat. Chem. Biol. 11

(2015) 309–315. doi:10.1038/nchembio.1789.
[168] M. Andersson, G. Chen, M. Otikovs, M. Landreh, K. Nordling, N. Kronqvist, P. Westermark, H. Jörnvall, S. Knight, Y. Ridderstråle, L. Holm, Q. Meng, K. Jaudzems, M. Chesler, J. Johansson, A. Rising, A. Holtzer, et al., Carbonic Anhydrase Generates CO2 and H+ That Drive Spider Silk Formation Via Opposite Effects on the Terminal Domains, PLoS Biol. 12 (2014) e1001921. doi:10.1371/journal.pbio.1001921.
[169] M. Widhe, U. Johansson, C.-O. Hillerdahl, M. Hedhammar, Recombinant spider silk with cell binding motifs for specific adherence of cells, Biomaterials. 34 (2013) 8223–8234. doi:10.1016/J.BIOMATERIALS.2013.07.058.
[170] F. Barnabé-Heider, K. Meletis, M. Eriksson, O. Bergmann, H. Sabelström, M.A. Harvey, H. Mikkers, J. Frisén, Genetic manipulation of adult mouse neurogenic niches by in vivo electroporation, Nat. Methods. 5 (2008) 189–196. doi:10.1038/nmeth.1174.
[171] B. Webb, B.J. Doyle, Parameter optimization for 3D bioprinting of hydrogels, Bioprinting. 8 (2017) 8–12. doi:10.1016/J.BPRINT.2017.09.001.
[172] T. Furusawa, H. Moribe, H. Kondoh, Y. Higashi, Identification of CtBP1 and CtBP2 as Corepressors of Zinc Finger-Homeodomain Factor δEF1, Mol. Cell. Biol. 19 (1999) 8581–8590. doi:10.1128/mcb.19.12.8581.
[173] D. Hübler, M. Rankovic, K. Richter, V. Lazarevic, W.D. Altrock, K.D. Fischer, E.D. Gundelfinger, A. Fejtova, Differential spatial expression and subcellular localization of CtBP family members in Rodent Brain, PLoS One. 7 (2012) e39710. doi:10.1371/journal.pone.0039710.
[174] C. Debiais-Delpech, J. Godet, N. Pedretti, F.X. Bernard, J. Irani, X. Cathelineau, O. Cussenot, G. Fromont, Expression patterns of candidate susceptibility genes HNF1β and CtBP2 in prostate cancer: Association with tumor progression, Urol. Oncol. Semin. Orig. Investig. 32 (2014) 426–432. doi:10.1016/j.urolonc.2013.09.006.
[175] F. Dai, Y. Xuan, J.-J. Jin, S. Yu, Z.-W. Long, H. Cai, X.-W. Liu, Y. Zhou, Y.-N. Wang, Z. Chen, H. Huang, CtBP2 overexpression promotes tumor cell proliferation and invasion in gastric cancer and is associated with poor prognosis., Oncotarget. 8 (2017) 28736–28749. doi:10.18632/oncotarget.15661.
[176] M. Götz, W.B. Huttner, The cell biology of neurogenesis, Nat Rev Mol Cell Biol. 6 (2005) 777–788. doi:10.1038/nrm1739.
[177] C. Englund, A. Fink, C. Lau, D. Pham, R.A.M. Daza, A. Bulfone, T. Kowalczyk, R.F. Hevner, Pax6, Tbr2, and Tbr1 are expressed sequentially by radial glia, intermediate progenitor cells, and postmitotic neurons in developing neocortex., J. Neurosci. 25 (2005) 247–51. doi:10.1523/JNEUROSCI.2899-04.2005.
[178] H. Liang, D.M. Fekete, O.M. Andrisani, CtBP2 Downregulation during Neural Crest Specification Induces Expression of Mitf and REST, Resulting in Melanocyte Differentiation and Sympathoadrenal Lineage Suppression, Mol. Cell. Biol. 31 (2011) 955–970. doi:10.1128/mcb.01062-10.
[179] O. Britanova, C. de Juan Romero, A. Cheung, K.Y. Kwan, M. Schwark, A. Gyorgy, T. Vogel, S. Akopov, M. Mitkovski, D. Agoston, N. ??estan, Z. Moln??r, V. Tarabykin, Satb2 Is a Postmitotic Determinant for Upper-Layer Neuron Specification in the Neocortex, Neuron. 57 (2008) 378–392. doi:10.1016/j.neuron.2007.12.028.
[180] J. Nan, S. Guan, X. Jin, Z. Jian, F. Linshan, G. Jun, Down-regulation of C-terminal binding protein 2 (CtBP2) inhibits proliferation, migration, and invasion of human SHSY5Y cells in vitro, Neurosci. Lett. 647 (2017) 104–109. doi:10.1016/j.neulet.2017.02.006.
[181] B. Martynoga, D. Drechsel, F. Guillemot, Molecular control of neurogenesis: A view from the mammalian cerebral cortex, Cold Spring Harb. Perspect. Biol. 4 (2012).

doi:10.1101/cshperspect.a008359.
[182] K. Zhang, L. Zhu, M. Fan, Oxygen, a Key Factor Regulating Cell Behavior during Neurogenesis and Cerebral Diseases, Front. Mol. Neurosci. 4 (2011) 5. doi:10.3389/fnmol.2011.00005.
[183] D. Stubbs, J. DeProto, K. Nie, C. Englund, I. Mahmud, R. Hevner, Z. Molnár, Neurovascular Congruence during Cerebral Cortical Development, Cereb. Cortex. 19 (2009) i32–i41. doi:10.1093/cercor/bhp040.
[184] L.-J. Zhao, Acetylation by p300 Regulates Nuclear Localization and Function of the Transcriptional Corepressor CtBP2, J. Biol. Chem. 281 (2006) 4183–4189. doi:10.1074/jbc.m509051200.
[185] I. van Leeuwen, S. Lain, Chapter 5 Sirtuins and p53, Adv. Cancer Res. 102 (2009) 171–195. doi:10.1016/S0065-230X(09)02005-3.
[186] T. Prozorovski, U. Schulze-Topphoff, R. Glumm, J. Baumgart, F. Schröter, O. Ninnemann, E. Siegert, I. Bendix, O. Brüstle, R. Nitsch, F. Zipp, O. Aktas, Sirt1 contributes critically to the redox-dependent fate of neural progenitors, Nat. Cell Biol. 10 (2008) 385–394. doi:10.1038/ncb1700.
[187] S.M. Gustafsdottir, E. Schallmeiner, S. Fredriksson, M. Gullberg, O. Söderberg, M. Jarvius, J. Jarvius, M. Howell, U. Landegren, Proximity ligation assays for sensitive and specific protein analyses, Anal. Biochem. 345 (2005) 2–9. doi:10.1016/J.AB.2005.01.018.
[188] Metabolic regulation of SIRT1 transcription via a HIC1: CtBP corepressor complex, (n.d.).
[189] S.S.C. Thio, J. V Bonventre, S.I.H. Hsu, The CtBP2 co-repressor is regulated by NADH-dependent dimerization and possesses a novel N-terminal repression domain, Nucleic Acids Res. 32 (2004) 1836–1847. doi:10.1093/nar/gkh344.
[190] C. Wang, Z. Tang, Y. Zhao, R. Yao, L. Li, W. Sun, Three-dimensional in vitro cancer models: a short review., Biofabrication. 6 (2014) 022001. doi:10.1088/1758-5082/6/2/022001.
[191] S. Kintzios, I. Yiakoumetis, G. Moschopoulou, O. Mangana, K. Nomikou, A. Simonian, Differential effect of the shape of calcium alginate matrices on the physiology of immobilized neuroblastoma N2a and Vero cells: A comparative study, Biosens. Bioelectron. 23 (2007) 543–548. doi:10.1016/J.BIOS.2007.07.003.
[192] T. Billiet, E. Gevaert, T. De Schryver, M. Cornelissen, P. Dubruel, The 3D printing of gelatin methacrylamide cell-laden tissue-engineered constructs with high cell viability, Biomaterials. 35 (2014) 49–62. doi:10.1016/J.BIOMATERIALS.2013.09.078.
[193] K. Nair, M. Gandhi, S. Khalil, K.C. Yan, M. Marcolongo, K. Barbee, W. Sun, Characterization of cell viability during bioprinting processes, Biotechnol. J. 4 (2009) 1168–1177. doi:10.1002/biot.200900004.
[194] Z. Bayoussef, J.E. Dixon, S. Stolnik, K.M. Shakesheff, Aggregation promotes cell viability, proliferation, and differentiation in an *in vitro* model of injection cell therapy, J. Tissue Eng. Regen. Med. 6 (2012) e61–e73. doi:10.1002/term.482.
[195] R.L. Mauck, C.C.-B. Wang, E.S. Oswald, G.A. Ateshian, C.T. Hung, The role of cell seeding density and nutrient supply for articular cartilage tissue engineering with deformational loading., Osteoarthr. Cartil. 11 (2003) 879–90.
[196] M. Andersson, Q. Jia, A. Abella, X.Y. Lee, M. Landreh, P. Purhonen, H. Hebert, M. Tenje, C. V Robinson, Q. Meng, G.R. Plaza, J. Johansson, A. Rising, Biomimetic spinning of artificial spider silk from a chimeric minispidroin, Nat. Chem. Biol. 13 (2017) 262–264. doi:10.1038/nchembio.2269.
[197] S. Wu, J. Johansson, P. Damdimopoulou, M. Shahsavani, A. Falk, O. Hovatta, A. Rising, Spider silk for xeno-free long-term self-renewal and differentiation of human pluripotent stem cells., Biomaterials. 35 (2014) 8496–8502.

doi:10.1016/j.biomaterials.2014.06.039.
[198] J.L. Bays, K.A. DeMali, Vinculin in cell–cell and cell–matrix adhesions, Cell. Mol. Life Sci. 74 (2017) 2999–3009. doi:10.1007/s00018-017-2511-3.
[199] W. Xu, H. Baribault, E.D. Adamson, Vinculin knockout results in heart and brain defects during embryonic development., Development. (1998). doi:10.1371/journal.pone.0011530.
[200] Y. Fan, G. Abrahamsen, R. Mills, C.C. Calderó, J.Y. Tee, L. Leyton, W. Murrell, J. Cooper-White, J.J. Mcgrath, A. Mackay-Sim, Focal Adhesion Dynamics Are Altered in Schizophrenia, Biol. Psychiatry. 74 (2013) 418–426. doi:10.1016/j.biopsych.2013.01.020.